



## FULL PAPER

# Quinoline-based promising anticancer and antibacterial agents, and some metabolic enzyme inhibitors

Salih Ökten<sup>1</sup> | Ali Aydın<sup>2</sup> | Ümit M. Koçyiğit<sup>3</sup> | Osman Çakmak<sup>4</sup> | Sultan Erkan<sup>5</sup> | Cenk A. Andac<sup>6</sup> | Parham Taslimi<sup>7</sup> | İlhami Gülçin<sup>8</sup>

<sup>1</sup>Department of Maths and Science Education, Kırıkkale University, Yahşihan, Kırıkkale, Turkey

<sup>2</sup>Department of Basic Medical Science, Faculty of Medicine, Yozgat Bozok University, Yozgat, Turkey

<sup>3</sup>Department of Basic Pharmacy Sciences, Faculty of Pharmacy, Cumhuriyet University, Sivas, Turkey

<sup>4</sup>Department of Gastronomy, Faculty of Arts and Design, Istanbul Rumeli University, Silivri, Istanbul, Turkey

<sup>5</sup>Department of Chemistry and Chemical Processing Technologies, Yıldızeli Vocational School, Sivas Cumhuriyet University, Sivas, Turkey

<sup>6</sup>Department of Pharmaceutical Chemistry, Faculty of Pharmacy, Istanbul Istinye University, Zeytinburnu, Istanbul, Turkey

<sup>7</sup>Department of Biotechnology, Faculty of Science, Bartın University, Bartın, Turkey

<sup>8</sup>Department of Chemistry, Faculty of Sciences, Atatürk University, Erzurum, Turkey

**Correspondence**

Salih Ökten, Department of Maths and Science Education, Kırıkkale University, Yahşihan, 71451 Kırıkkale, Turkey.

Email: [salihokten@kku.edu.tr](mailto:salihokten@kku.edu.tr);

[sokten@gmail.com](mailto:sokten@gmail.com)

**Abstract**

A series of substituted quinolines was screened for their antiproliferative, cytotoxic, antibacterial activities, DNA/protein binding affinity, and anticholinergic properties by using the 3-(4,5-dimethylthiazol-2-yl)-2,5-diphenyltetrazolium bromide cell proliferation, lactate dehydrogenase cytotoxicity, and microdilution assays, the Wolfe–Shimmer equality method, the Ellman method, and the esterase assay, respectively. The results of the cytotoxic and anticancer activities of the compounds displayed that 6-bromotetrahydroquinoline (**2**), 6,8-dibromotetrahydroquinoline (**3**), 8-bromo-6-cyanoquinoline (**10**), 5-bromo-6,8-dimethoxyquinoline (**12**), the novel *N*-nitrated 6,8-dimethoxyquinoline (**13**), and 5,7-dibromo-8-hydroxyquinoline (**17**) showed a significant antiproliferative potency against the A549, HeLa, HT29, Hep3B, and MCF7 cancer cell lines ( $IC_{50} = 2\text{--}50\ \mu\text{g/ml}$ ) and low cytotoxicity ( $\sim 7\text{--}35\%$ ) as the controls, 5-fluorouracil and cisplatin. The compound–DNA linkages are hyperchromic or hypochromic, causing variations in their spectra. This situation shows that they can be bound to DNA with the groove-binding mode, with  $K_b$  value in the range of  $2.0 \times 10^3\text{--}2.2 \times 10^5\ \text{M}^{-1}$ . Studies on human Gram(+) and Gram(–) pathogenic bacteria showed that the substituted quinolines exhibited selective antimicrobial activities with MIC values of 62.50–250  $\mu\text{g/ml}$ . All tested quinoline derivatives were found to be effective inhibitors of acetylcholinesterase (AChE) and the human carbonic anhydrase I and II isoforms (hCA I and II), with  $K_i$  values of 46.04–956.82 nM for hCA I, 54.95–976.93 nM for hCA II, and 5.51–155.22 nM for AChE. As a result, the preliminary data showed that substituted quinolines displayed effective pharmacological features. Molecular docking studies were performed to investigate the binding modes and interaction energies for compounds **2–17** with AChE (PDB ID: 4EY6), hCA I (PDB ID: 1BMZ), and hCA II (PDB ID: 2ABE).

**KEYWORDS**

acetylcholinesterase enzyme inhibition, antibacterial, anticancer activity, carbonic anhydrase enzyme inhibition, DNA binding, molecular docking, quinolone

**1 | INTRODUCTION**

Cancer leads to an uncontrolled cell growth to invade other tissues and organs by spreading to the body through the blood. Despite the

intensive work on effective cancer treatment, it is an enormous life-threatening problem for human health in the world, as 11 million people have been affected from cancer in the world and unfortunately, seven million people have died due to cancer.<sup>[1]</sup>

Nowadays, many scientists have made efforts to cure cancer or reduce its occurrence. Although many anticancer drugs have been developed for the treatment of cancer, these drugs have some limitations, such as side effects, tumor specificity, and tumor cell resistance.<sup>[2]</sup> Thus, the developments of new anticancer drug candidates without side effects are necessary as alternatives to current chemotherapeutic drugs.<sup>[3]</sup>

Quinoline heterocycles, developing rapidly, as well as their synthetic versatility,<sup>[4]</sup> are a highly attractive ring system in organic chemistry due to their usage in developing new compounds possessing a wide range of biological activities.<sup>[5–10]</sup> Furthermore, the quinoline scaffold is widespread in natural products and drugs, and it is considered an important pharmacophore and a privileged structure in medicinal chemistry.<sup>[11]</sup> Particularly, anticancer drugs bearing the quinoline nucleus led to an increase in their anticancer activities through different mechanisms involving apoptosis, cell cycle arrest, and inhibition of angiogenesis.<sup>[12]</sup> Moreover, the substantial anticancer activities of several quinoline analogs through DNA intercalation, causing interference in the replication, have been reported.<sup>[9]</sup> Despite the fact that a considerable number of biological, synthetic, and semisynthetic quinolines, having important pharmacological roles, have been reported in the literature, available methods for preparation of synthetic quinoline derivatives starting from quinoline pharmacophore are restricted.<sup>[13–15]</sup>

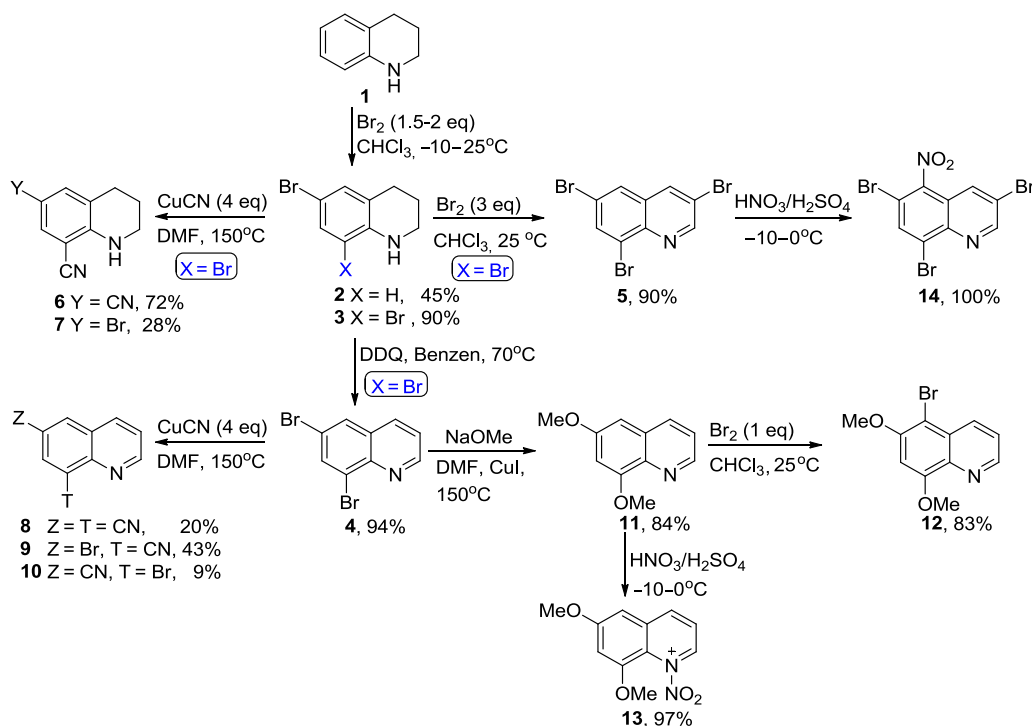
Many studies about pharmacological features of aryl or nitro/amino-substituted quinolines have been interested due to that they have been starting materials for bioactive polycyclic systems.<sup>[16,17]</sup> Nitrated derivatives, which exhibit biological potency, that is, antileishmanial<sup>[18]</sup> or potent mutagenic activities,<sup>[19]</sup> are important key compounds for the preparation of amino derivatives for pharmacological use.<sup>[16,20]</sup> The aryl-substituted quinolines displayed a high antipesticide activity against the nematode *Haemonchus contortus*,<sup>[21]</sup> agricultural predatory activity, significant antibacterial activity,<sup>[22]</sup> anti-inflammatory, analgesic, antipyretic activities, and efficient inhibition of the COX-2 enzyme.<sup>[23]</sup> Moreover, a series of substituted 2-phenylquinolines exhibited a superior ER $\beta$  affinity in a cell-based transcriptional assay,<sup>[24]</sup> potent antiplatelet activities,<sup>[25]</sup> antimetabolic activity,<sup>[26]</sup> and antiproliferative activity against HCT-116 (colon cancer), MCF7 (breast cancer), and MDA-MB-435 (breast cancer) with low GI<sub>50</sub> values.<sup>[27]</sup>

As halogen has a crucial role in the bioactivity of compounds and provides an avenue for further structure elaboration, halogen-containing quinolines are of particular interest.<sup>[28]</sup> Bromoquinolines are an important class of precursors for preparing heterocyclic compounds with multifunctionality.<sup>[7,29,30]</sup> These building blocks have especially been used within medicinal chemistry as starting materials for numerous compounds with a pharmacological activity.<sup>[7]</sup> Bromoquinolines have attracted more and more attention in drug discovery due to their potential to make halogen bonds. Halogen atoms are typically located at the circumference of organic molecules and are positioned to be involved in intermolecular interactions.<sup>[31]</sup> A halogen bond (XB), a highly versatile and specific interaction that behaves similar to the classical

hydrogen bond (HB), is formed between a covalently bonded halogen atom (e.g., C–X, X = Cl, Br, I; XB donor) and a nucleophile (i.e., Lewis base; XB acceptor). Due to that the halogen bond has attracted great attention in recent years, with hit-to-lead and lead-to-candidate optimization aiming to increase drug-target binding affinity optimization. Generally, heavy organohalogens (i.e., organochlorines, organobromines, and organoiodines) are capable of forming halogen bonds, whereas organofluorines are not capable of doing so.<sup>[32]</sup>

Cyano-substituted quinolines have important roles in biological systems. Notably, quinoline compounds bearing cyano group at the C-3 position can act to deactivate the action of growth factor receptor protein tyrosine kinases.<sup>[33]</sup> Agents with cyano groups also bind with biological systems as small molecule inhibitors.<sup>[34]</sup> The most common strategies for preparation of quinolines are cyclization reactions of *N*-functionalized benzene or cyclohexane.<sup>[35]</sup> The 2-cyano-substituted dihydro- and tetrahydroquinolines have been synthesized using the Reissert reaction,<sup>[36]</sup> whereas 8-cyano-substituted quinoline compounds have been prepared by the treatment of cyano aniline with ketone-functionalized alkynes in polar solvents.<sup>[37]</sup> Due to this, the cyclizations using cyano-substituted *N*-functionalized aromatics allow only the synthesis of monocyano-substituted quinolines,<sup>[38]</sup> and the synthesis of polycyano-substituted quinolines has been restricted. However, we have accomplished di- or tricyano-substituted quinolines by substitution strategy to be used multipurpose, especially as a drug.<sup>[39]</sup>

Previously, brominated quinolines, the starting compounds, were synthesized according to reported procedures starting from 1,2,3,4-tetrahydroquinoline and 8-hydroxyquinoline,<sup>[8,30,40]</sup> followed by transformation to their respective cyano, methoxy, phenyl, and amino derivatives.<sup>[7,14,17,39]</sup> The antiproliferative activity of 6,8-dibromotetrahydroquinoline and 5,7-dibromo-8-hydroxyquinoline against several cancer cell lines was determined by the BrdU cell proliferation enzyme-linked immunosorbent assay (BCPE).<sup>[6–8]</sup> The results showed that 6,8-dibromotetrahydroquinoline and 5,7-dibromo-8-hydroxyquinoline significantly inhibited proliferation of HeLa, C6, and HT29 cells, as compared with 5-fluorouracil (5-FU) at 5  $\mu$ g/ml and higher concentrations. Recently, the synthesized 6-bromo-5-nitroquinoline<sup>[20]</sup> has been observed to exhibit a high biological activity, with antiproliferative, cytotoxic, and apoptotic effects on several cancer cell lines.<sup>[15]</sup> Due to their inhibitory potency against cancer cell lines, several bromo, nitro, methoxy, and nitrile derivatives were prepared by starting from 6,8-dibromotetrahydroquinoline and 5,7-dibromo-8-hydroxyquinoline according to procedures in the literature reported by our group.<sup>[15]</sup> In this study, we focused on the determination of anticancer activity against different cancer cell lines, antibacterial activity against some Gram(+) and Gram(–) microorganisms and acetylcholinesterase (AChE), and carbonic anhydrase enzyme inhibition potentials of these derivatives. In addition, the activity of the substituted quinolines against AChE and human carbonic anhydrase I and II isoform (hCA I and II) metabolic enzymes was supported by molecular docking studies.



**SCHEME 1** A schematic presentation of substituted quinolines 2–14, starting with 1,2,3,4-tetrahydroquinoline (1)

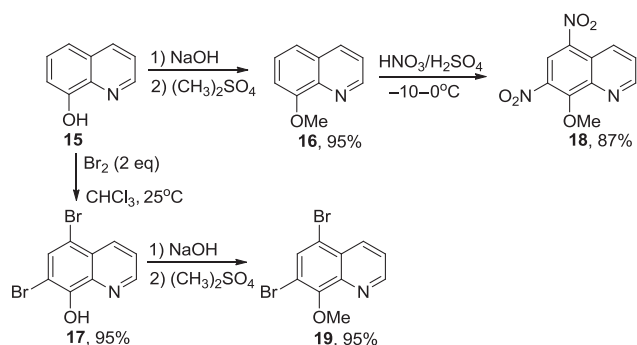
## 2 | RESULTS AND DISCUSSION

### 2.1 | Chemistry

In our previous studies, brominated quinoline derivatives, 6,8-dibromotetrahydroquinoline (**3**) and 6,8-dibromoquinoline (**4**), were converted to corresponding nitrile derivatives (**6**–**10**) by treatment of CuCN according to our reported procedures (Scheme 1).<sup>[6,39]</sup> Moreover, in our reported studies, the treatment of 6,8-dibromoquinoline (**4**) with NaOCH<sub>3</sub> furnished 6,8-dimethoxyquinoline (**11**).<sup>[6]</sup> Then, 5-bromo-6,8-dimethoxyquinoline (**12**) was obtained by bromination of 6,8-dimethoxyquinoline (**11**) according to reported procedure (Scheme 1).<sup>[14]</sup> The direct nitration of 6,8-dimethoxyquinoline (**11**) with HNO<sub>3</sub>/H<sub>2</sub>SO<sub>4</sub> mixture resulted in the formation of a novel 6,8-dimethoxy-1-nitroquinoline (N-nitrated) (**13**) as sole product in a high yield (97%; Scheme 2). 8-Methoxyquinoline (**16**) was prepared by treatment of 8-hydroxyquinoline (**15**) with NaOH and (CH<sub>3</sub>)<sub>2</sub>SO<sub>4</sub> at 0–80°C in 95% yield. Then, the novel dinitrate 8-methoxyquinoline was obtained by the direct nitration of 8-methoxyquinoline (**16**) with HNO<sub>3</sub>/H<sub>2</sub>SO<sub>4</sub> mixture as the sole product in a high yield (87%; Scheme 2). 3,6,8-Tribromoquinoline (**5**) was nitrated with a mixture of HNO<sub>3</sub>/H<sub>2</sub>SO<sub>4</sub> at 0°C. The reaction yielded quantitatively 3,6,8-bromo-5-nitroquinoline (**14**) as the sole product (Scheme 1).

The structures of nitrate-containing compounds **13** and **18** were determined by <sup>1</sup>H NMR (nuclear magnetic resonance), <sup>13</sup>C NMR, Fourier transform infrared (FT-IR), and elemental analysis. In the <sup>1</sup>H NMR spectrum of **18**, the characteristic doublet of doublet for H-2 of the quinoline scaffold was observed at 9.17 ppm (<sup>4</sup>J = 1.6 Hz and

<sup>3</sup>J = 4.0 Hz). The signals for the aromatic protons H-3 and H-4 ( $\delta_{\text{H}}$  7.84, <sup>3</sup>J = 4.4 Hz and <sup>3</sup>J = 8.8 Hz; 9.22, <sup>4</sup>J = 1.6 Hz and <sup>3</sup>J = 8.8 Hz, respectively) were shifted more downfield when compared with signals of the starting material. The proton of the benzene ring of **18** gave a singlet downfield at  $\delta_{\text{H}}$  8.89, assigning bromine to C-6. It was seen that the signals of H-5 and H-7 disappeared after nitration, when compared with signal systems of the starting material **16**, which is evidence for the existence of nitration at both C-5 and C-7 positions. The <sup>1</sup>H NMR signals of coupled compound **13** had the same signal system as starting material **11**, but signals of protons were observed further downfield. In the <sup>1</sup>H NMR spectra of **14**, signals of H-2 and H-4 were observed as a doublet at  $\delta_{\text{H}}$  9.12 and 8.24 (<sup>4</sup>J = 2.0 Hz), respectively, downfield as compared with chemical shifting values of starting molecule **5**.<sup>[39]</sup> Moreover, the



**SCHEME 2** A schematic presentation of substituted quinolines 16–19, starting with 8-hydroxyquinoline (15)

disappearance of the H-5 doublet signal of the starting material **5**<sup>[39]</sup> at  $\delta_{\text{H}}$  8.14 and the appearance of a singlet signal at  $\delta_{\text{H}}$  8.33 can be possible evidence of NO<sub>2</sub> group bounded to C-5 position. In the FT-IR spectra of 3,6,8-bromo-5-nitroquinoline (**14**), characteristic N=O stretching signals were observed at 1,550 and 1,320 cm<sup>-1</sup>.

## 2.2 | Biological activity

### 2.2.1 | Antiproliferative activities of the compounds

Many anticancer drug candidates have been withdrawn from market due to their serious side effects, loss of sensitivity to drugs, and limited use for many cancer types. The anticancer activities of quinoline derivatives were reported in many works. In our recent studies,<sup>[6-8,15]</sup> the antiproliferative activities of 6,8-dibromo-1,2,3,4-tetrahydroquinoline (**3**), 5,7-dibromo-8-hydroxyquinoline (**17**), 6-bromo-8-cyano-1,2,3,4-tetrahydroquinoline, and nitrated 3,6,8-tribromoquinoline (**5**) against HeLa, HT29, and C6 cell lines using sulforhodamine-B stain (SRB) and BCPE assays were determined. In the present study, the substituted quinoline derivatives (Table 1) were prepared according to reported procedures<sup>[6,30,39-42]</sup> by our research group and investigated for their anticancer effects and cytotoxicities against the A549 HeLa, Hep3B, HT29, MCF7, and FL cell lines using the 3-(4,5-dimethylthiazol-2-yl)-2,5-diphenyltetrazolium

bromide (MTT) protocol. Growth inhibition (GI<sub>50</sub>), total growth inhibition (TGI), and lethal concentration (LC<sub>50</sub>) parameters of the compounds were evaluated according to the NCI screening method, and half-maximal inhibitory concentrations (IC<sub>50</sub>) of these molecules were calculated using Four-Parameter Logistic Function. When TGI and IC<sub>50</sub> values of the compounds were examined, it was found that tested compounds exhibited selective antitumor properties against all tested cell lines (Tables 1 and 2).

When TGI and IC<sub>50</sub> values of the compounds were examined, it was observed that 8-bromo-6-cyanoquinoline (**10**) had the strongest antitumor effect against all tested cell lines, with IC<sub>50</sub> values ranging between 1.5 and 22.5 µg/ml in a series of nitrile quinolines (Table 1 and 2). Whereas 6-bromo-8-cyanoquinoline (**9**) and 6,8-dicyanotetrahydroquinoline (**6**) showed a good antiproliferation activity against only one cell line, A549 (IC<sub>50</sub> = 5.4 µg/ml) and HT29 (IC<sub>50</sub> = 78.1 µg/ml), respectively, 6-bromo-8-cyanotetrahydroquinoline (**7**) and 6,8-dicyanoquinoline (**8**) did not show inhibition against any tested cancer cell lines (Table 1 and 2). Our previous results obtained by SRB assay<sup>[15]</sup> confirmed that 6-bromo-8-cyanotetrahydroquinoline (**7**) did not display an antiproliferative activity against HeLa and HT29 cells.

In a series of bromoquinolines, 6-bromotetrahydroquinoline (**2**) and 6,8-dibromotetrahydroquinoline (**3**) significantly inhibited the proliferation of all tested cancer cell lines, except A549, with IC<sub>50</sub> values ranging between 3.7 and 48.5 µg/ml. Whereas 6,8-dibromoquinoline (**4**) displayed an inhibition activity against only

**TABLE 1** GI<sub>50</sub>, TGI, LC<sub>50</sub>, and IC<sub>50</sub> of the test compounds against A549, FL, and HeLa cells

Compounds (µg/ml)	A549				FL				HeLa			
	GI <sub>50</sub>	TGI	LC <sub>50</sub>	IC <sub>50</sub>	GI <sub>50</sub>	TGI	LC <sub>50</sub>	IC <sub>50</sub>	GI <sub>50</sub>	TGI	LC <sub>50</sub>	IC <sub>50</sub>
<b>2</b>	6.1	>1,000	>1,000	435.2	4.2	27.6	>1,000	27.1	2.0	4.3	19.8	4.3
<b>3</b>	5.6	511.9	>1,000	206.3	4.1	16.8	312.7	16.6	1.7	3.6	19.4	3.7
<b>4</b>	>1,000	>1,000	>1,000	>1,000	3.3	314.4	>1,000	288.1	5.7	317.8	>1,000	295.4
<b>5</b>	169.3	>1,000	>1,000	>1,000	4.2	>1,000	>1,000	>1,000	9.7	>1,000	>1,000	>1,000
<b>6</b>	372.5	>1,000	>1,000	>1,000	4.3	>1,000	>1,000	>1,000	7.1	>1,000	>1,000	>1,000
<b>7</b>	>1,000	>1,000	>1,000	>1,000	3.7	213.2	>1,000	198.8	8.1	>1,000	>1,000	912.5
<b>8</b>	18.5	>1,000	>1,000	>1,000	3.1	39.7	>1,000	38.2	12.8	>1,000	>1,000	>1,000
<b>9</b>	1.9	6.8	255.4	5.4	3.1	>1,000	>1,000	>1,000	3.9	>1,000	>1,000	>1,000
<b>10</b>	4.9	29.1	>1,000	22.5	2.1	7.3	207.8	7.2	1.7	4.3	47.3	4.3
<b>12</b>	31.2	>1,000	>1,000	>1,000	4.5	51.7	>1,000	50.3	4.2	18.9	396.7	18.7
<b>13</b>	308.1	>1,000	>1,000	>1,000	3.7	28.9	>1,000	28.3	5.1	52.7	>1,000	51.2
<b>14</b>	>1,000	>1,000	>1,000	>1,000	3.3	25.3	>1,000	24.6	3.1	11.2	178.9	11.1
<b>17</b>	2.0	7.3	240.9	5.8	3.4	17.9	960.6	17.6	4.4	18.9	361.1	18.7
<b>18</b>	10.1	>1,000	>1,000	>1,000	3.7	32.6	>1,000	31.8	7.5	>1,000	>1,000	>1,000
<b>19</b>	>1,000	>1,000	>1,000	>1,000	2.9	288.9	>1,000	262.5	5.3	159.4	>1,000	151.4
Cisplatin				60.5				52.8				50.3
5-FU				69.8				59.1				61.6

Abbreviations: 5-FU, 5-fluorouracil; GI, growth inhibition; IC, inhibition concentration; LC, lethal concentration; TGI, total growth inhibition.

**TABLE 2** GI<sub>50</sub>, TGI, LC<sub>50</sub>, and IC<sub>50</sub> of the test compounds against Hep3B, HT29, and MCF7 cells

Compounds (µg/ml)	Hep3B				HT29				MCF7			
	GI <sub>50</sub>	TGI	LC <sub>50</sub>	IC <sub>50</sub>	GI <sub>50</sub>	TGI	LC <sub>50</sub>	IC <sub>50</sub>	GI <sub>50</sub>	TGI	LC <sub>50</sub>	IC <sub>50</sub>
2	5.2	49.6	>1,000	48.5	4.1	26.6	>1,000	21.8	2.8	20.7	>1,000	19.8
3	5.4	41.9	>1,000	41.1	2.6	9.3	199.2	7.9	3.7	19.8	926.9	19.3
4	3.1	38.8	>1,000	37.4	1.2	>1,000	>1,000	>1,000	1.9	402.3	>1,000	309.2
5	3.8	958.4	>1,000	831.1	2.5	>1,000	>1,000	>1,000	1.7	>1,000	>1,000	>1,000
6	7.5	>1,000	>1,000	>1,000	1.4	557.2	>1,000	78.1	2.5	>1,000	>1,000	>1,000
7	5.5	>1,000	>1,000	>1,000	2.5	>1,000	>1,000	>1,000	2.6	>1,000	>1,000	>1,000
8	4.6	>1,000	>1,000	>1,000	3.1	>1,000	>1,000	894.5	1.3	>1,000	>1,000	>1,000
9	5.5	>1,000	>1,000	>1,000	1.6	>1,000	>1,000	465.9	2.4	927.2	>1,000	683.6
10	2.3	5.6	36.2	5.6	1.1	1.7	11.2	1.5	1.7	4.8	66.5	4.6
12	3.9	78.2	>1,000	74.7	2.9	26.1	>1,000	19.2	2.3	84.8	>1,000	75.6
13	4.1	22.7	>1,000	22.3	4.5	39.0	>1,000	30.1	2.9	20.4	>1,000	19.5
14	4.4	200.9	>1,000	186.8	2.9	7.6	50.9	7.1	2.5	8.7	154.0	8.5
17	3.4	66.5	>1,000	62.7	1.9	6.5	227.6	5.4	2.4	17.5	>1,000	16.5
18	3.5	18.6	849.7	18.3	3.8	>1,000	>1,000	>1,000	2.4	23.7	>1,000	22.3
19	6.0	>1,000	>1,000	>1,000	6.2	>1,000	>1,000	>1,000	2.5	>1,000	>1,000	>1,000
Cisplatin				48.7				40.4				63.8
5-FU				62.9				65.2				74.2

Abbreviations: 5-FU, 5-fluorouracil; GI, growth inhibition; IC, inhibition concentration; LC, lethal concentration; TGI, total growth inhibition.

Hep3B (IC<sub>50</sub> = 37.4 µg/ml; TGI = 38.8 µg/ml), 3,6,8-tribromoquinoline (5) did not exhibit any antitumoral activity against any cancer cell lines. However, nitrated derivative of tribromoquinoline (5) showed a significant antiproliferative activity against FL, HeLa, HT29, and MCF7 (IC<sub>50</sub> values ranging from 7.1 to 24.6 µg/ml; TGI ranging from 7.6 to 25.3 µg/ml). The results of significant antiproliferative activities of 6,8-dibromotetrahydroquinoline (3) and 5-nitro-3,6,8-tribromoquinoline (14) against HeLa and HT29 were confirmed by our previous results obtained by SRB and BCPE assays.<sup>[6,7,15]</sup>

We have obtained interesting results on antiproliferative effects of substituted hydroxy- and methoxyquinoline derivatives. Our previous study<sup>[6]</sup> showed that 5,7-dibromo-8-hydroxyquinoline (17) exhibited a strong anticancer activity against HeLa, HT29, and C6 cancer cell lines by SRB and BCPE assays. MTT assay also confirmed its significant effect against HeLa and HT29 cells (IC<sub>50</sub> = 18.7 and 5.4 µg/ml; TGI = 18.9 and 6.5 µg/ml, respectively). Moreover, 5,7-dibromo-8-hydroxyquinoline displayed a significant antiproliferative activity against A549, Hep3B, and MCF7 cancer cell lines and FL healthy cells (with IC<sub>50</sub> values ranging between 5.8 and 62.7 µg/ml; TGI values ranging between 7.3 and 66.5 µg/ml). Interestingly, 5,7-dibromo-8-methoxyquinoline (19) derived from 5,7-dibromo-8-hydroxyquinoline (17) did not inhibit proliferation of any cancer cell lines. However, compound 18 bearing nitro group instead of bromine in the same positions of 5,7-dibromo-8-methoxyquinoline (19) depicted a selective inhibitory activity against Hep3B and MCF7 cells (IC<sub>50</sub> = 18.3 and 22.3 µg/ml; TGI = 18.6 and

23.7 µg/ml, respectively). 6,8-Dimethoxyquinoline (4) exhibited a selective antiproliferative activity against only HT29 cell lines.<sup>[6]</sup> In this study, brominated 12 and N-nitrated 13 at C-5 forms of 6,8-dimethoxyquinoline (11) inhibited proliferation of all studied cancer cells, except A549, with IC<sub>50</sub> values ranging from 19.2 to 75.6 µg/ml (Table 2). When the IC<sub>50</sub> and TGI values of all the abovementioned compounds are considered, effective ones have better or similar antiproliferative effects compared with the positive control group, cisplatin and 5-FU (Table 3). In addition, the active compounds can be used in advanced pharmacological studies when low GI<sub>50</sub> values (~1–5 µg/ml) and high LC<sub>50</sub> values (200 to >1,000 µg/ml) are considered (Table 1 and 2). Overall, the GI<sub>50</sub>, TGI, and LC<sub>50</sub> parameters of the respective molecules are at the desired level and meet the NCI criteria.

## 2.2.2 | Cytotoxic activity of compounds and the morphological changes in cancer cell lines

It is important for a substance to have a minimal toxicity against normal cells. For this reason, antitumor and cytotoxic properties of these compounds should be compared to find the forward pharmacological capacity of each. The cytotoxicities of the compounds in cells were tested by the lactate dehydrogenase (LDH) assay, indirectly demonstrating membrane damage. When the measurement results of cytoplasmic LDH activity are evaluated for these

**TABLE 3** Minimum inhibitory concentrations (MIC, in µg/ml) of the compounds

Compounds	<i>Enterococcus faecalis</i> (ATCC 19433)	<i>E. faecalis</i> (ATCC 29212)	<i>Staphylococcus aureus</i> (ATCC 25923)	<i>S. aureus</i> (ATCC 29213)	<i>S. aureus</i> (ATCC 46300)	<i>Escherichia coli</i> (ATCC 25922)	<i>E. coli</i> (ATCC 35218)	<i>Pseudomonas eruginosa</i> (ATCC 27853)
2	500	1,000	1,000	500	250	500	1,000	1,000
4	500	1,000	>1,000	500	125	1,000	1,000	>1,000
5	250	500	1,000	500	500	>1,000	>1,000	>1,000
6	1,000	1,000	>1,000	500	500	1,000	>1,000	>1,000
7	500	1,000	500	1,000	1,000	1,000	1,000	1,000
8	500	1,000	>1,000	250	500	1,000	1,000	>1,000
9	1,000	1,000	>1,000	250	125	1,000	1,000	>1,000
10	1,000	1,000	500	500	500	500	1,000	500
12	125	500	1,000	125	62.5	500	1,000	1,000
13	500	1,000	250	250	250	1,000	1,000	500
14	500	1,000	1,000	500	125	1,000	1,000	500
18	125	125	125	125	125	500	500	500
19	125	500	1,000	500	250	1,000	1,000	1,000
SCF	250	62.5	250	62.5	250	15.62	31.25	250

Abbreviations: ATCC, American Type Culture Collection; SCF, sulbactam (30 µg) + cefoperazone (75 µg), as a positive control.

compounds, it has been found that compounds **6**, **8**, **9**, **12**, **13**, and **19** for A549 cancer cells; **7**, **10**, **13**, **14**, and **19** for Hep3B cancer cells; **4**, **5**, **6**, **9**, **12**, **17**, and **19** for MCF7 cells; **4**, **5**, **8**, **9**, and **18** for HeLa cells; **4**, **5**, **6**, **7**, **8**, **9**, **18**, and **19** for HT29 cells; and **2**, **3**, **13**, **14**, **17**, and **19** for FL cells cause approximately 7–19% membrane damage at their IC<sub>50</sub> concentration (Figure 1). If the compounds are compared with controls (5-FU and cisplatin) for this evaluation, the toxicity of molecules mentioned above is very close to the cytotoxicity values of 5-FU and cisplatin. Therefore, they may be suitable for advanced pharmacological assays (Figure 1).

To investigate the morphology of cell-treated compounds, we used compound **3**. When the effects of **3** used at 20 µg/ml concentration on A549, Hep3B, HT29, MCF7, and FL cell morphology were visualized, some changes were observed in the cells using phase-contrast microscopy. As shown in Figure 2, each cell line exposed to compound **3** exhibited a low cell confluence, floating cells, cellular and cytoplasmic shrinkage, cytoplasmic extensions of bubble, and clumping of cells together. The morphological change most likely indicates the apoptotic process. Moreover, the effect of substituted quinoline derivatives at 20-µg/ml concentration on cells was so small that it did not change the normal appearance of the cells, maintaining a normal morphology.

### 2.2.3 | Antibacterial activities of the compounds

The effects of the compounds on some pathogenic bacteria causing disease in the human body have been evaluated using the minimum inhibition concentration (MIC) method. We considered our test molecules to be antibacterial at 250 µg/ml and below the MIC values. The MIC values of the compounds were compared with the values of

antimicrobial drug (SCF = sulbactam [30 µg] + cefoperazone [75 µg]) used as positive controls. When the MIC values of newly synthesized molecules displayed on Gram(+) bacteria were examined, it was found that antibacterial effects of compounds **5**, **12**, **18**, and **19**

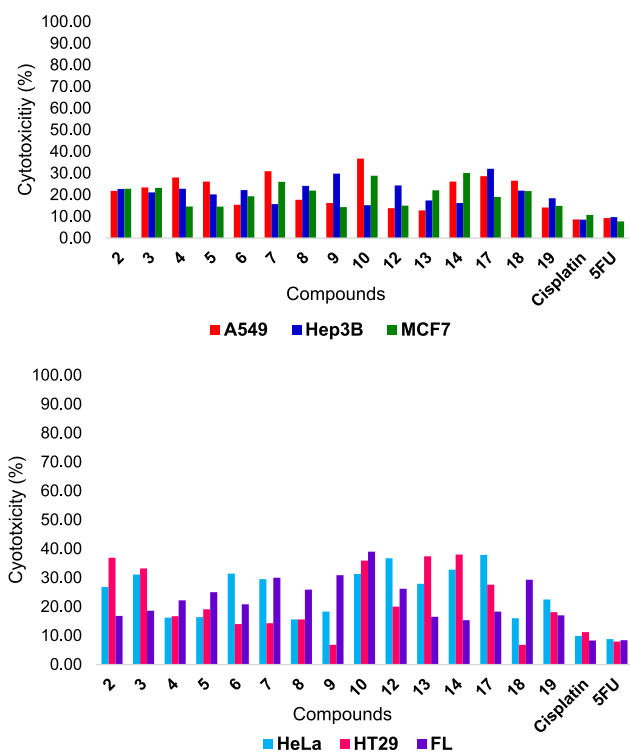


**FIGURE 1** % Cytotoxicity of these compounds and positive controls against A549, Hep3B, MCF7, HeLa, HT29, and FL cells at IC<sub>50</sub> concentrations

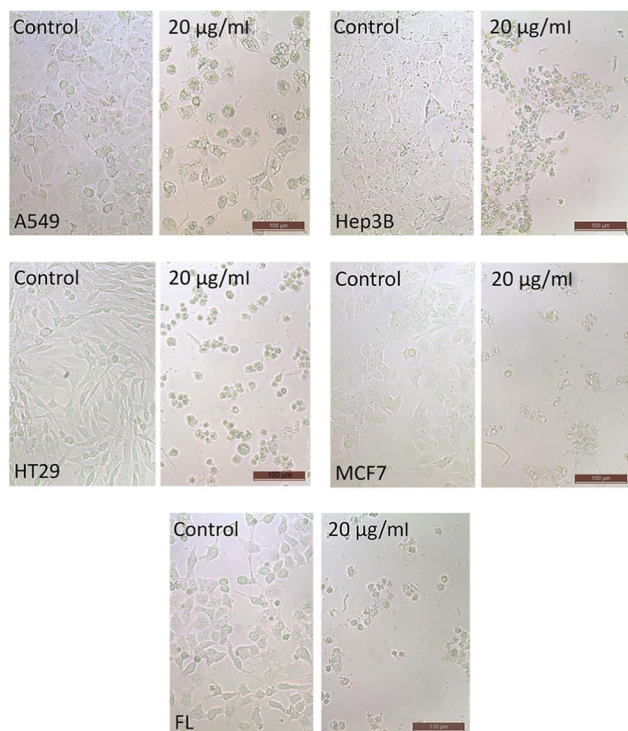


**FIGURE 2** The effect of compound **3** on the morphologies of A549, Hep3B, HT29, MCF7, and FL cells. Exponentially growing cells were incubated overnight with 20 µg/ml of compound **3** at 37°C. Control cells were treated with only dimethyl sulfoxide. All measurements were 100 µm

against *Enterococcus faecalis* (VRE) ATCC 19433 (MIC values ranging from 125 to 250 µg/ml), only compound **18** against *E. faecalis* ATCC 29212 (MIC = 125 µg/ml), compounds **13** and **18** against *Staphylococcus aureus* ATCC 25923 (values ranging from 125 to 250 µg/ml), compounds **8**, **9**, **12**, **13**, and **18** against *S. aureus* (MSSA) ATCC 29213 (MIC values ranging from 125 to 250 µg/ml), compounds **2**, **4**, **9**, **12**, **13**, **14**, **18**, and **19** against *S. aureus* MRSA ATCC 46300 (62.5–250 µg/ml) were more or similar to the SCF antibiotic used as a positive control (Table 3). According to the MIC values exhibited by the synthesized molecules on Gram(–) bacteria, it was found that none of our molecules had a sufficiently strong antibacterial effect on the *Escherichia coli* ATCC 25922, *E. coli* ATCC 35218, and *P. aeruginosa* ATCC 27853 strain (Table 3).

## 2.2.4 | DNA binding properties of the compounds

DNA binding properties of the compounds were determined using the ultraviolet (UV)–visible absorption (Vis) spectrophotometer. Binding type and binding constants of the compounds were explained as follows. A single maximum absorption peak was observed in the spectrum of **4**, **6**, **7**, **9**, **10**, **12**, **14**, and **19**, and no clear redshifts or blueshifts on this peak were observed. When circulating tumor DNA (CT-DNA) was added in an increasing amount to the reaction mixture, the reduction in the absorption intensity of molecules **9** and **12** resulted in a

hypochromic effect, and the increase in the absorption intensity of molecules **4**, **5**, **6**, **7**, **8**, **10**, **13**, **14**, **18**, and **19** caused a hyperchromic appearance (Figure 3). The binding constants ( $K_b$ ) of the compounds show the affinity of the complex to DNA with the aid of the following Wolfe–Shimmer equality equation:  $[DNA]/(\epsilon a - \epsilon f) = [DNA]/(\epsilon b - \epsilon f) + 1/K_b(\epsilon b - \epsilon f)$ , where the  $[DNA]$  symbol is the DNA concentration in the base pairs and the  $\epsilon a$ ,  $\epsilon f$ , and  $\epsilon b$  symbols are the molar absorption coefficients of the  $A_{observed}/[Compound]$ , free compound, and compound–DNA solutions, respectively.  $K_b$  is the binding constant that is related to the affinity between the compound and DNA, and it can be calculated algebraically from the slope of the line drawn between  $[DNA]/(\epsilon a - \epsilon f)$  and  $[DNA]$ . When the binding constants given in Table 4 are evaluated, it can be seen that the  $K_b$  values of the compounds are between  $2.0 \times 10^3$  and  $2.2 \times 10^5 \text{ M}^{-1}$ . The binding constants of the molecules in this group are ordered from large to small as follows: **18** > **7** > **6** > **8** > **4** > **14** > **12** > **5** > **9** > **13** > **10** > **19**. When the data in Table 4 are examined, it is understood that **18** binds DNA much more strongly than others. However, the binding constants of the **17**, **2**, and **3** could not be calculated using UV–Vis spectrophotometric method.

## 2.2.5 | Metabolic enzyme inhibition activity

### Anti-AChE activity results

We have reported the inhibitory activity against AChE of substituted quinoline derivatives and of control compound, tacrine ( $IC_{50} = 224.93 \text{ nM}$  for AChE) in Table 1, expressed as  $IC_{50}$  values. The substituted quinoline derivatives, **2**–**10**, **12**–**14**, and **17**–**18**, were found to be potent inhibitor compounds of cholinesterases with  $IC_{50}$  in the nanomolar concentration scale. The excellent AChE inhibitors in the assayed series of substituted quinoline analogs are all tested cyanoquinoline derivatives **7**, **6**, **8**, and **10**, except **9** ( $IC_{50} = 111.34 \text{ nM}$ ), and novel *N*-nitrate 6,8-dimethoxyquinoline **13** with  $IC_{50}$  values ranging between 6.84 and 26.94 nM. 6-Bromotetrahydroquinoline (**2**) and 3,6,8-tribromoquinoline (**5**) significantly inhibited AChE enzyme at  $IC_{50}$  values of 47.94 and 88.95 nM, respectively, whereas 6,8-dibromotetrahydroquinoline (**3**;  $IC_{50} = 101.53 \text{ nM}$ ) and its aromatic form **4** ( $IC_{50} = 136.19 \text{ nM}$ ) showed a moderate inhibition against AChE enzyme, compared with tacrine (Table 5). The quinoline derivatives **17**–**19** substituted at C-5, C-7, and C-8, respectively, showed a better inhibition than tacrine against AChE with an  $IC_{50}$  range of 72.23–104.23 nM.

### Carbonic anhydrases inhibition activity results

An esterase assay method<sup>[41,42]</sup> was used to investigate the inhibition potentials of substituted quinoline derivatives against two physiologically relevant CA isoforms, the slower cytosolic isoform (hCA I) and the more rapid cytosolic isoenzyme (hCA II). In this assay, acetazolamide (AZA) was used as a standard drug due to its utilization in clinical application as a carbonic anhydrase inhibitor. CA I and II isoforms' inhibition data of compounds are summarized and their  $IC_{50}$  and  $K_i$  values expressed in nanomolar (nM) range are displayed in Table 6.

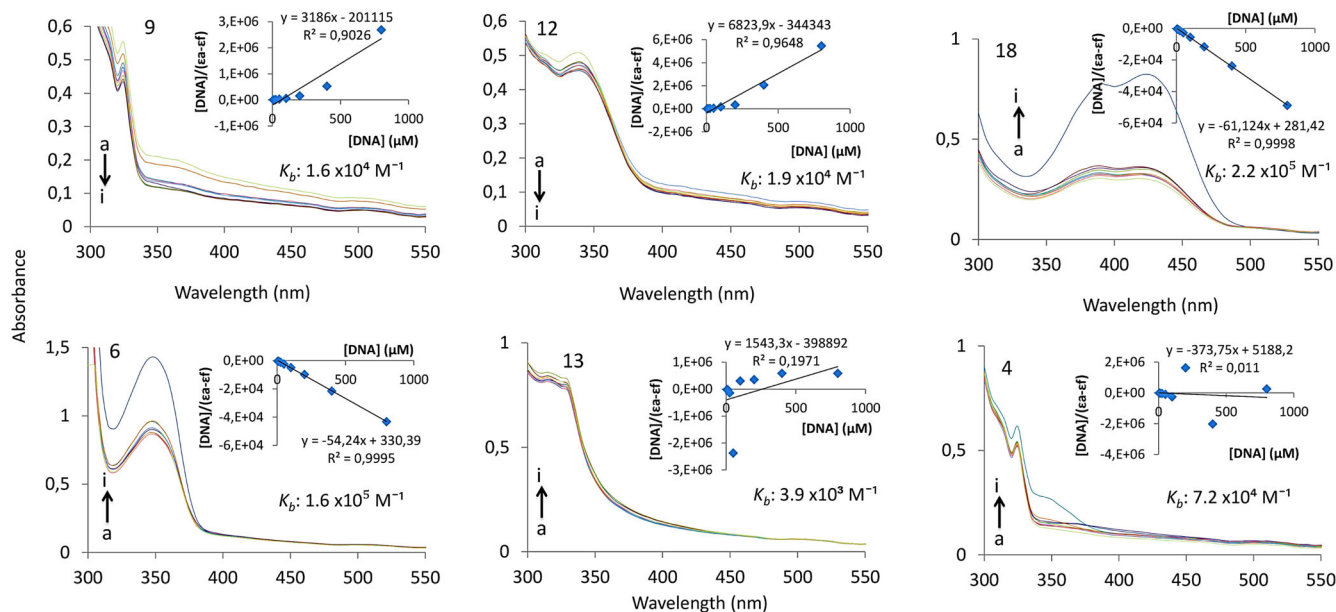


**FIGURE 3** Ultraviolet-visible absorption spectra of 25- $\mu\text{M}$  selected compounds in the absence (a) and presence of 6.25  $\mu\text{M}$  (b), 12.5  $\mu\text{M}$  (c), 25  $\mu\text{M}$  (d), 50  $\mu\text{M}$  (e), 100  $\mu\text{M}$  (f), 200  $\mu\text{M}$  (g), 400  $\mu\text{M}$  (h), and 800  $\mu\text{M}$  (i) DNA. The direction of the arrow demonstrates increasing concentrations of DNA. Inside graph is the plot of  $[\text{DNA}]$  versus  $[\text{DNA}]/(\epsilon a - \epsilon f)$  to find the binding constant of the complex-DNA adduct

Most of the substituted quinoline analogs remarkably inhibited the slow cytosolic isoform hCA I, taking part in important physiological and pathological processes in many tissues and organs,<sup>[43]</sup> with  $K_i$  values ranging between 39.52 and 574.52 nM. 6,8-Dicyanotetrahydroquinoline (**6**) and 5,7-dibromo-8-methoxyquinoline (**19**) were determined as the best inhibitors for this isoform, with  $K_i$  values of 39.52 and 48.05 nM, respectively. The *N*-nitrated (**13**) and brominated 6,8-dimethoxyquinoline (**12**) at C-5 and their starting material, 6,8-dibromoquinoline (**4**), have displayed a significant inhibition against cytosolic isoform hCA I with a  $K_i$  value range of 103.64  $\pm$  20.63–125.50  $\pm$  14.78 nM (Table 6). Moreover, for 5-acetamido-1,3,4-thiadiazole-2-sulfonamide (AZA), a broad-specificity CA inhibitor and used for the treatment of altitude sickness, cystinuria, idiopathic intracranial hypertension, glaucoma, and epileptic seizure, a  $K_i$  value of 1,005.47  $\pm$  75.60 nM was recorded against hCA I. The high concentration of the hCA II led to several diseases such as glaucoma, osteoporosis, and renal tubular acidosis.<sup>[41]</sup> Against rapid cytosolic isoenzyme hCA II, substituted quinoline analogs (**2–10**, **12–14**, and **17–13**) had  $K_i$  values ranging

**TABLE 4** The binding constants ( $K_b$ ) of these compounds

Compound	$K_b$ ( $\text{M}^{-1}$ )	Compound	$K_b$ ( $\text{M}^{-1}$ )
4	$7.2 \times 10^4$	10	$3.0 \times 10^3$
5	$1.8 \times 10^4$	12	$1.9 \times 10^4$
6	$1.6 \times 10^5$	13	$3.9 \times 10^3$
7	$1.6 \times 10^5$	14	$2.2 \times 10^4$
8	$7.3 \times 10^4$	18	$2.2 \times 10^5$
9	$1.6 \times 10^4$	19	$2.0 \times 10^3$

from 54.95 to 976.93 nM. The inhibitory potentials of substituted quinoline derivatives against the hCA II had a similar behavior to that against hCA I. In addition, AZA had a medium inhibition potential against this isoform, with a  $K_i$  value of 1,104.43 nM.

**TABLE 5** Acetylcholinesterase (AChE) inhibitory activity ( $\text{IC}_{50}$  and  $K_i$ ) of the substituted quinoline derivatives

Compounds	$\text{IC}_{50}$ (nM)		$K_i$ (nM)
	AChE	$r^2$	AChE
2	47.94	0.9376	40.14 $\pm$ 7.94
3	101.53	0.9593	92.83 $\pm$ 13.05
4	136.19	0.9818	95.73 $\pm$ 20.88
5	88.95	0.9533	75.04 $\pm$ 13.94
6	23.94	0.9952	20.91 $\pm$ 4.08
7	15.03	0.9572	12.95 $\pm$ 3.41
8	26.94	0.9491	20.15 $\pm$ 2.94
9	111.34	0.9593	90.45 $\pm$ 16.94
10	6.84	0.9583	5.51 $\pm$ 0.94
12	176.03	0.9596	155.22 $\pm$ 26.37
13	16.04	0.9882	12.88 $\pm$ 2.93
14	95.26	0.9815	69.05 $\pm$ 9.35
17	104.23	0.9911	83.22 $\pm$ 14.06
18	72.73	0.9390	61.15 $\pm$ 8.58
19	88.20	0.9106	75.52 $\pm$ 17.90
Tacrine <sup>a</sup>	224.93	0.9880	187.66 $\pm$ 33.61

Note: The results were expressed in nanomolar (nM) range.

<sup>a</sup>Tacrine was used as a standard inhibitor for AChE enzyme.

**TABLE 6** The enzyme inhibition results of substituted quinoline analogs against human carbonic anhydrase isoenzymes I and II (hCA I and II)

Compounds	IC <sub>50</sub> (nM)		K <sub>i</sub> (nM)			
	hCA I	r <sup>2</sup>	hCA II	r <sup>2</sup>	hCA I	hCA II
2	804.02	0.9583	1,004.85	0.9889	956.82 ± 104.80	976.93 ± 105.80
3	1,005.80	0.9374	834.93	0.9583	926.33 ± 82.64	963.33 ± 95.35
4	83.04	0.9490	105.94	0.9588	103.64 ± 20.63	119.05 ± 13.94
5	394.63	0.9374	486.77	0.9375	408.84 ± 45.93	514.86 ± 57.04
6	39.52	0.9485	52.84	0.9460	46.04 ± 8.63	54.95 ± 5.93
7	406.92	0.9284	409.75	0.9355	444.28 ± 68.84	417.04 ± 73.80
8	507.27	0.9372	496.33	0.9905	635.33 ± 71.26	684.03 ± 88.31
9	281.52	0.9733	333.84	0.9911	306.82 ± 58.04	335.96 ± 42.07
10	305.04	0.9804	397.01	0.9799	294.62 ± 21.74	304.75 ± 65.66
12	101.88	0.9882	144.76	0.9550	125.50 ± 14.78	157.11 ± 30.51
13	93.05	0.9918	106.83	0.9485	104.94 ± 11.66	115.94 ± 21.95
14	285.02	0.9084	304.88	0.9856	350.73 ± 54.93	394.02 ± 94.85
17	288.90	0.9309	318.63	0.9646	347.91 ± 18.66	385.18 ± 83.85
18	574.52	0.9406	507.73	0.9496	663.06 ± 92.06	582.33 ± 85.03
19	48.05	0.9923	67.04	0.9930	51.68 ± 5.95	61.05 ± 4.77
AZA <sup>a</sup>	1,103.70	0.9586	1,188.01	0.9691	1,005.47 ± 75.60	1,104.43 ± 95.55

Note: The results were expressed in nanomolar (nM) range.

<sup>a</sup>Acetazolamide (AZA) was used as a standard inhibitor for each hCA I and II enzymes.

## 2.3 | Docking studies

### 2.3.1 | Docking analyses for enzyme inhibition

For different substituted quinoline derivatives **1–19**, the inhibitory activity was determined by a molecular simulation method against AChE, hCA I, and hCA II enzymes. The estimated free energies of binding obtained from molecular docking results, which is a kind of molecular simulation method, are listed for **1–19** in Table 7. In addition, to determine the activity against the AChE enzyme and hCA I and hCA II enzymes of a chemical species, tacrine, and AZA, respectively, which were taken as a reference, were docked with the relevant target proteins.

The inhibition efficiency of each compound and reference substances against selected target proteins is listed in Table 7. According to Table 7, the obtained docking results and the experimental IC<sub>50</sub> values are quite compatible with each other. Also, it was found that the estimated free energies of binding values of the compounds without IC<sub>50</sub> values in Tables 5 and 6 were lower than the energies of the relevant reference substances. Compound **10** has the highest activity with  $-6.90$  kcal/mol binding energy against the 4EY6 target protein determined for the AChE enzyme. The studied compounds exhibited a similar activity against proteins selected for hCA I and hCA II enzymes. When the molecular docking and experimental inhibition efficacy are compared, the only difference between molecular simulation and experimental results can be seen in compounds **6** and **8** against 4EY6. Unlike experimental IC<sub>50</sub> values, the estimated

**TABLE 7** The estimated free energy of binding (kcal/mol) between the test compounds and target proteins

Compounds	4EY6	1BMZ	2ABE
2	-5.24	-4.85	-4.05
3	-4.53	-4.60	-4.08
4	-4.23	-5.65	-5.77
5	-4.83	-5.26	-4.62
6	-6.00	-5.94	-5.95
7	-6.80	-5.05	-4.55
8	-6.58	-4.95	-4.51
9	-4.47	-5.40	-4.86
10	-6.90	-5.30	-4.87
12	-3.71	-5.51	-4.84
13	-6.77	-5.54	-4.93
14	-2.78	-5.39	-4.64
17	-2.86	-5.37	-4.70
18	-4.94	-4.94	-4.30
19	-4.92	-5.87	-5.86
Tacrine	-3.53	-	-
Acetazolamide	-	-4.18	-3.92

free energies of binding values of **8** are greater than that of **6**, which may be due to secondary chemical interactions between the compounds and amino acid residues of the target proteins. Compound **8** formed more H-bonds with the amino acid residues of the protein than **6**. Due to this status, the binding energy of compound **8** may have been more. It can also be incorporated into the nonbonded electron pair resonance structure on the nitrogen atom in compound **8**, and this nitrogen atom has a less steric effect than compound **6**.

The binding modes between amino acid residues of the first five compounds (these compounds are written in red in Tables 5 and 6) with a high activity against 4EY6, 2ABE, and 1BMZ proteins are given in Figure 4.

### 2.3.2 | Docking analyses for an anticancer effect of compound 10

In an attempt to look into the mechanism of action of compound **10**, we extensively searched through the SEA receptor database ([sea.bkslab.org](http://sea.bkslab.org)),<sup>[44]</sup> which gave rise to a highly potential target, phospholipase C gamma 1 (PLC $\gamma$ 1). PLC $\gamma$ 1, which is overexpressed in many metastatic tumors,<sup>[44–47]</sup> is involved in the generation of second messengers from phosphatidylinositol 4,5-bisphosphate (PIP<sub>2</sub>) to signal cell proliferation and differentiation.<sup>[48]</sup> The downregulation (or inhibition) of PLC $\gamma$ 1 in nude mice was reported to essentially suppress lung metastasis.<sup>[47]</sup> The inhibition of PLC $\gamma$ 1 by small molecules such as

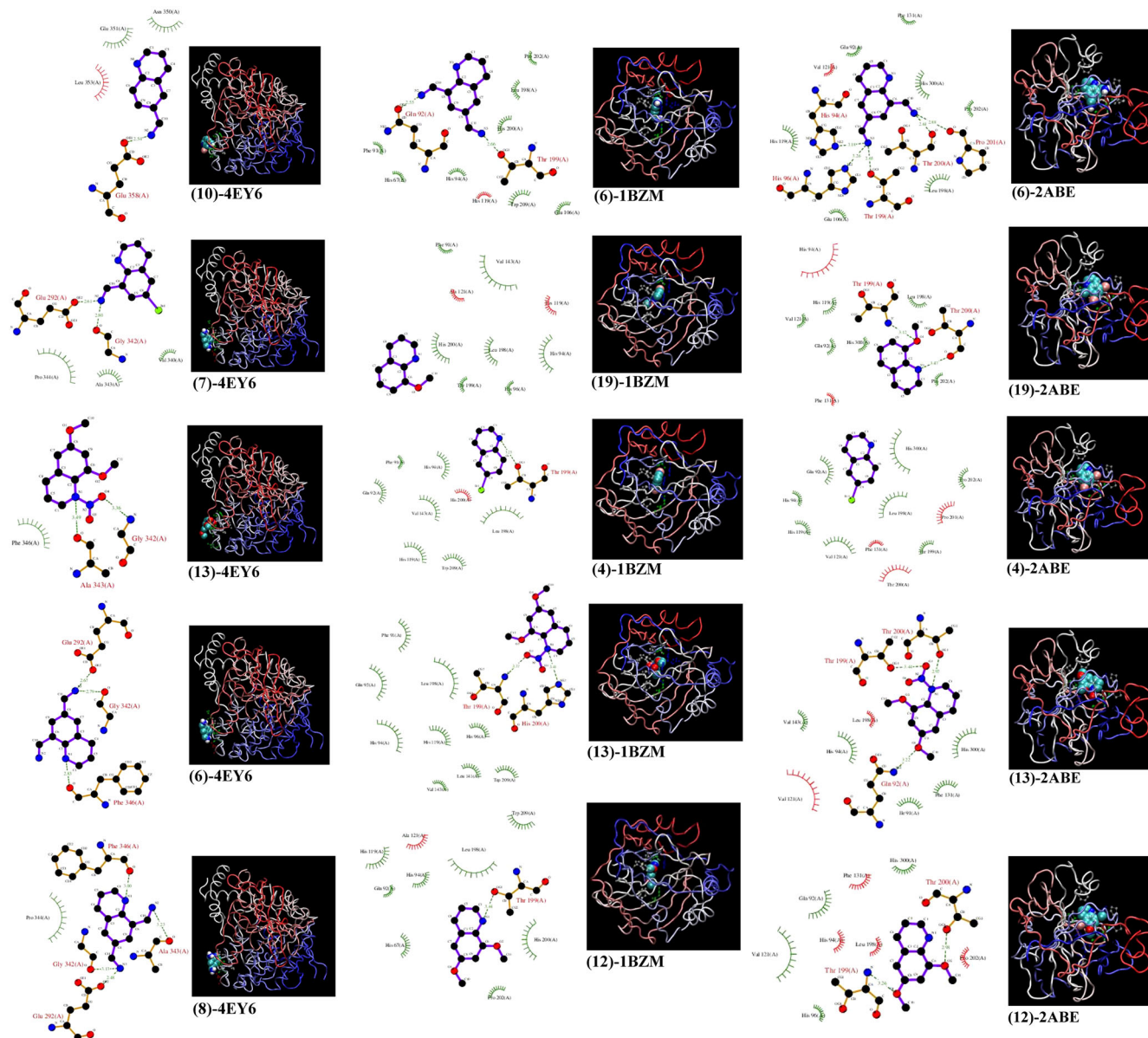


**FIGURE 4** Docking poses of the five most active inhibitors of each target protein

triterpene esters<sup>[49]</sup> was reported to diminish cancer cell proliferation. It was also reported that some sulfonylpyridinediamine derivatives<sup>[50]</sup> inhibit PLC $\gamma$ 1 at submicromolar concentrations. Furthermore, the inhibition of PLC $\gamma$ 1 was reported to induce autophagy in human colon cancer and hepatocellular carcinoma cells, which was mediated by downstream interference with the mTOR/ULK1 pathway as well as dissociation of the beclin1-IP3R-Bcl-2 complex.<sup>[51]</sup>

Recently, it has been experimentally confirmed that the small molecule binding site of the PLC $\gamma$ 1 complex structure is in the nSH2 domain that binds the phosphorylated tyrosine 766 (pY766) residue of the tyrosine kinase domain of growth factors.<sup>[52]</sup> Therefore, DOCK studies were performed on an X-ray structure of nSH2 in complex with fibroblast growth factor receptor 2 (FGFR2; PDB ID: 5EG3).<sup>[53]</sup> As seen in Figure 5a,b, compound **10** suitably and favorably docks into the FGFR2 binding site of PLC $\gamma$ 1. Apparently, binding of compound **10** prevents a sequence LEU(774)ASP(771)LEU(772)SER(773)GLN(774) of FGFR2 from binding, significantly diminishing the binding interactions between PLC $\gamma$ 1 and FGFR2. Binding of **10** in the binding site of nSH2 of PLC $\gamma$ 1 is highly likely to prevent the phosphorylated TYR(769) residue of FGFR2 to conduct its kinase activity on PLC $\gamma$ 1. To the best of authors' knowledge, there are only a few small molecule inhibitors of PLC $\gamma$ 1 published in literature. Therefore, we propose that compound **10** could represent a potential drug candidate, which should be further investigated for metastatic cancer treatment.

## 2.4 | The structure-activity relationship study

The determination of antiproliferative effects of the substituents on quinoline cycle indicated that the presence of bromine and cyano groups at positions C-6 and C-8 in compounds **4** and **8** did not inhibit the proliferation of cancer cell lines, and also three bromine groups bound at C-3, C-6, and C-8 in compound **5** did not increase the antiproliferative activity. The nitration of **5** at C-5 led to show a selective antiproliferation activity against HeLa, MCF7, and HT29 cell lines ( $IC_{50}$  = 11.1, 8.5, and 7.1  $\mu$ g/ml, respectively). In particular, the nitro

group at C-5 of **14** is critical for an antiproliferative activity. Compound **4** bearing bromine at C-6 and C-8 exhibits a selective antiproliferative activity against Hep3B cells ( $IC_{50}$  = 37.4  $\mu$ g/ml). Moreover, the cyano group substituted at C-6 in **4** resulted in having significant inhibition potentials of **10** against all tested cancer cell lines. However, the presence of nitrile at C-8 for quinoline bromides, that is, compound **9**, showed a selective inhibition against only A549 cells ( $IC_{50}$  = 5.4  $\mu$ g/ml). On the contrary, bromination of 1,2,3,4-tetrahydroquinoline (**1**) at C-6 and C-8 in compounds **2** and **3** has increased antiproliferative activities against MCF7, HT29, Hep3B, and HeLa cell lines with  $IC_{50}$  values of 3.7 and 48.5  $\mu$ g/ml, except A549 cells. However, the strong antiproliferative activity of 6,8-dibromotetrahydroquinoline (**3**) significantly reduced against tested cancer cell lines in case of cyano groups exchanged at C-6 and/or C-8 in compounds **6** and **7**. Our previous study<sup>[7]</sup> reported that the methoxy group bound at both C-6 and C-8 in a quinoline cycle showed a selective inhibition against HT29 cells, whereas bromination at C-5 or nitration at N-1 positions of this compound led to display an antiproliferation activity against MCF7, HT29, Hep3B, HeLa, and FL cell lines. 8-Hydroxyquinoline (**15**) brominated at C-5 and C-7 has a strong inhibition of proliferation of all tested cell lines with  $IC_{50}$  values of 5.4 and 62.7  $\mu$ g/ml. However, the reduction in significant inhibition of compound **19** indicated that the methoxy group replaced the hydroxy group at C-8, which significantly decreased inhibition potential of **19**. Interestingly, 8-methoxyquinoline nitrated at C-5 and C-7 displayed a selective antiproliferation effect against MCF7, Hep3B, and FL cell lines with  $IC_{50}$  values of 22.3, 18.3, and 31.8  $\mu$ g/ml, respectively. According to these results, it can be concluded that the cyano group bound at C-6 and hydroxy group bound at C-8 for quinoline bromides (**10** and **17**) and bromination at C-5 and nitration of N atom of 6,8-dimethoxyquinoline (**12** and **13**) led to significantly increased inhibition potentials against cancer cell lines, but the presence of cyano and methoxy groups at C-8 for quinoline bromides (**6-8** and **19**) reduced the inhibition activity.

When the MIC values of substituted quinolines displayed on Gram(+) bacteria were examined, it was observed that some of the compounds had a selective antibacterial effect. Whereas **5** showed an antibacterial effect against only *E. faecalis* (VRE) ATCC 19433

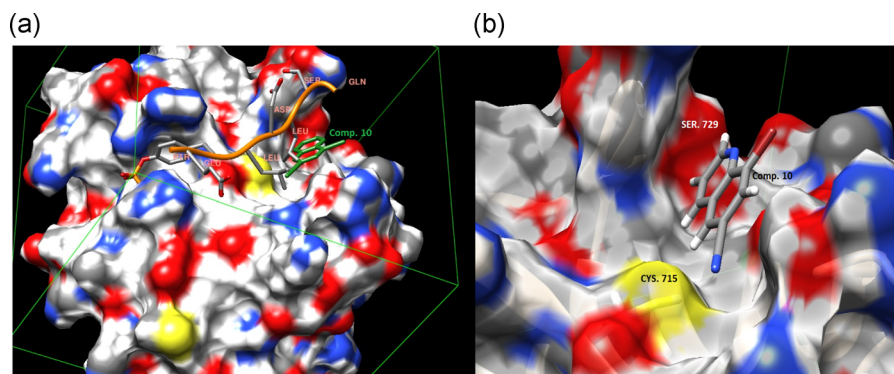


**FIGURE 5** The docked structure of compound **10** in complex with the X-ray structure coordinates of PLC $\gamma$ 1 (PDB ID: 5EG3).<sup>[53]</sup> (a) X-ray structure coordinates of a small FGFR2 peptide (PDB ID: 5EG3) and docked coordinates of **10** are both shown, and (b) only the docked coordinates of **10** are shown in the binding site of PLC $\gamma$ 1. P-TYR(769) in (a) is phosphorylated TYR residue of FGFR2, which phosphorylates nSH2 to activate PLC $\gamma$ 1

(125 µg/ml of MIC value), **2**, **4**, and **14** had an antibacterial effect only against *S. aureus* ATCC 46300 (MIC = 250, 125, and 125 µg/ml, respectively). Compound **18** displayed an inhibitory activity against all tested Gram(+) bacteria at an MIC value of 125 µg/ml; however, it did not have a sufficient antibacterial effect against all tested Gram(-) bacteria. Whereas **13** showed an antibacterial effect against *S. aureus* ATCC 25923, *S. aureus* ATCC 29213 (MSSA), and *S. aureus* ATCC 46300 at an MIC value of 250 µg/ml, **10**, **6**, and **7** did not have any antibacterial effect against tested Gram(+) and Gram(-) bacteria. Against *E. faecalis* ATCC 19433, **12**, **18**, and **19** (MIC = 125 µg/ml) had a better antibacterial effect than the control compound (SCF, MIC = 250 µg/ml). Against *S. aureus* ATCC 46300, **12** had the strongest inhibition at an MIC value of 62.5 µg/ml, compared with all tested compounds and positive control (SCF; MIC = 250 µg/ml; Table 4). Moreover, **9**, **4**, **14**, and **18** had a stronger effect (MIC = 125 µg/ml) against *S. aureus* ATCC 46300, compared with positive control (SCF; MIC = 250 µg/ml; Table 4). Against *E. faecalis* ATCC 29212, only **18** displayed an antibacterial effect. In brief, against tested Gram(+) bacteria, substituted quinolines have a moderate antibacterial effect. However, these compounds did not show inhibition against any Gram(-) bacteria. It is evident that both the nature and position of the substituents for different substituted quinoline derivatives are able to cause variation in the AChE, cytosolic hCA I, and hCA II enzyme inhibition activities of quinoline. All quinoline derivatives have good inhibitory activities against AChE, cytosolic hCA I, and hCA II enzymes, compared with standard compounds, tacrine and AZA, respectively. Although the selectivity and variation of the above-mentioned enzyme inhibition potentials of substituted quinolines were not observed, their anticancer and antibacterial activities showed that substituted quinoline analogs had selective antiproliferative and antibacterial effects. For example, **7**, **6** (except for its antiproliferative activity against HT29; IC<sub>50</sub> = 78.1 µg/ml), and **8** (except for its antiproliferative activity against A549; IC<sub>50</sub> = 5.4 µg/ml) did not display antiproliferation against tested cancer cell lines and antibacterial activities on tested Gram(+) and Gram(-) bacteria, whereas these compounds significantly inhibited AChE ( $K_i$  = 12.95, 20.15, 20.91, and 90.45 nM, respectively), cytosolic hCA I ( $K_i$  = 444.28, 635.33, 46.04, and 306.82 nM, respectively), and hCA II ( $K_i$  = 417.04, 684.03, 54.95, and 335.96 nM, respectively) enzymes. Moreover, **10** exhibited the highest antiproliferative activities against all tested cancer cell lines (IC<sub>50</sub> values ranging from 1.5 to 22.5 µg/ml) and high enzyme inhibitory effect against AChE ( $K_i$  = 5.51 nM), hCA I ( $K_i$  = 296.62 nM), and hCA II ( $K_i$  = 304.75 nM), compared with standard compounds. However, this molecule exhibited an antibacterial activity against only *S. aureus* ATCC 46300 (MIC = 125 µg/ml). According to these results, it can be concluded that nitrile group at the positions of C-6 and C-8 or only C-8 of quinoline cycle decreased the anticancer activity and antibacterial effects, whereas the presence of nitrile group in quinoline cycle enhanced the enzyme inhibition against AChE, cytosolic hCA I, and hCA II. However, the nitrile group bound at only C-6 promoted antiproliferation against cancer cell lines in addition to enzyme inhibitory activity.

Similarly, brominated quinolines, 3,6,8-tribromoquinoline (**5**), 5,7-dibromo-8-methoxyquinoline (**19**), and 6,8-dibromoquinoline (**4**), except its antiproliferative effect against Hep3B; IC<sub>50</sub> = 37.4 µg/ml), did not show any anticancer and antibacterial effect. However, these compounds inhibited AChE ( $K_i$  ranging from 75.04 to 95.73 µg/ml), cytosolic hCA I ( $K_i$  ranging from 51.68 to 408.84 µg/ml), and hCA II ( $K_i$  ranging from 61.05 to 514.86 µg/ml) enzymes. On the contrary, brominated tetrahydroquinoline derivatives, **2** and **3**, exhibited both anticancer activity and enzyme (AChE, hCA I, and hCA II) inhibitory potential.

The nitration of quinoline in any position led to increased enzyme inhibition, due to which **13**, **18**, and **14** had a significant enzyme inhibitory effect against AChE ( $K_i$  = 12.88, 61.15, and 69.05 nM, respectively), cytosolic hCA I ( $K_i$  = 104.94, 663.06, and 350.73 nM, respectively), and hCA II ( $K_i$  = 115.94, 582.33, and 394.02 nM, respectively).

### 3 | CONCLUSION

Recently synthesized substituted quinoline bearing different functional groups and novel nitrated methoxyquinoline analogs were tested for their antibacterial, anticancer activities in vitro, and enzyme inhibition effects. We have shown that substituted quinolines have a significant potential as enzyme inhibitors against AChE, hCA I, and hCA II, and also a selective anticancer effect against A549, HeLa, Hep3B, HT29, and MCF7 cancer cell lines. When TGI and IC<sub>50</sub> values of the compounds were examined, we found that 5,7-dibromo-8-hydroxyquinoline (**17**; IC<sub>50</sub> values between 5.4 and 62.7 µg/ml; TGI values between 6.5 and 66.5 µg/ml), 8-bromo-6-cyanoquinoline (**10**; IC<sub>50</sub> values between 1.5 and 22.5 µg/ml; TGI values between 1.7 and 29.1 µg/ml), 6,8-dibromotetrahydroquinoline (**3**; IC<sub>50</sub> values between 3.7 and 41.1 µg/ml; TGI values between 3.1 and 41.9 µg/ml, except A549 cell line), and novel synthesized N-nitrated 6,8-dimethoxyquinoline (**13**; IC<sub>50</sub> values between 19.5 and 51.2 µg/ml; TGI values between 20.4 and 52.7 µg/ml, except A549 cell line) have very strong antitumor effects against all tested cell lines (Table 1 and 2). All anticancer test results indicate that these compounds, especially **10**, can be promising anticancer agent candidates. Moreover, the docking study for anticancer activity suggested that **10** could represent a potential anticancer drug candidate for metastatic cancer treatment due to its potential to suppress the PLC $\gamma$ 1. Novel synthesized 5,7-dinitro-8-methoxyquinoline (**18**) has the potential of being an antibacterial agent against Gram(+) bacteria (MIC = 125 µg/ml). Also, all of the substituted quinolines effectively reduced enzyme activities of AChE, hCA I, and hCA II at the nanomolar concentrations. The substituted quinoline analogs can be drug candidates of the CAIs for therapy of some diseases such as epilepsy, osteoporosis, glaucoma, gastric and duodenal ulcers, neurological disturbances, and they can be drug candidates of the AChE inhibitor for the therapy of Alzheimer's disease. The activity of quinoline derivatives substituted with a number of different functional groups against AChE and human carbonic anhydrase isoenzymes (hCA I and

II) was supported by molecular docking studies. Experimental IC<sub>50</sub> results of the compounds against these enzymes were found to be highly compatible with each other.

## 4 | EXPERIMENTAL

### 4.1 | Chemistry

#### 4.1.1 | General

Thin-layer chromatography was carried out on Merck silica F254 0.255-mm plates, and spots were visualized by UV at 254 nm. Flash column chromatography was performed using Merck 60 (70–230 mesh) silica gel. The microwave reactions were run in CEM Discover Labmate instrument. Melting points were determined on a Thomas–Hoover capillary melting points apparatus. Solvents were concentrated at a reduced pressure. IR spectra were recorded on a Bruker Vertex 70 v FT-IR instrument. Mass spectra were recorded on a spectrometer under electron-impact (EI) and chemical ionization conditions. The elemental analysis was recorded on an ElementarVario MICRO Cube instrument. NMR spectra were recorded on Bruker 400 MHz for <sup>1</sup>H and at 100 MHz for <sup>13</sup>C NMR.

The original spectra of the novel compounds are provided as Supporting Information. The InChI codes of the investigated compounds are also provided as Supporting Information.

#### 4.1.2 | The synthesis of substituted quinoline compounds

This study was carried out with substituted quinolines **2–10**, **12–14**, and **17–19** according to our previous papers.<sup>[6,7,14,20,30]</sup> Moreover, two novel nitrated methoxyquinoline derivatives were synthesized for this paper. In brief, the synthesis of 6-bromo-1,2,3,4-tetrahydroquinoline (**2**), 6,8-dibromo-1,2,3,4-tetrahydroquinoline (**3**), and 3,6,8-tribromoquinoline (**5**) via direct bromination of 1,2,3,4-tetrahydroquinoline (**1**) and 6,8-dibromoquinoline (**4**) via aromatization of **3** with DDQ has been reported in our previous publications.<sup>[6,29,30,39,54]</sup> The cyano and methoxyquinoline derivatives (**6–11**) starting from 6,8-dibromo-1,2,3,4-tetrahydroquinoline (**3**) and 6,8-dibromoquinoline (**4**) treated with NaOMe or CuCN were synthesized according to our reported procedures.<sup>[14,39]</sup> Furthermore, the synthesis of 5,7-dibromo-8-hydroxyquinoline (**17**) and 5,7-dibromo-8-methoxyquinoline (**19**) via bromination of 8-hydroxyquinoline (**15**) and 8-methoxyquinoline (**16**), respectively, was reported in our recent works.<sup>[40,55]</sup> The isolated compounds, **2–10**, **12–14**, and **17–19**, were fully characterized by melting point, HRMS analysis, infrared, <sup>1</sup>H, <sup>13</sup>C, HMBC (heteronuclear multiple bond correlation), and HETCOR spectroscopy in these papers.<sup>[6,29,30,39,40,43]</sup> All tested compounds were purified by column chromatography. The purity of the tested compounds was monitored with <sup>1</sup>H NMR spectroscopy.

#### 4.1.3 | The synthesis of 5,7-dinitro-8-methoxyquinoline

8-Methoxyquinoline (**16**; 0.50 g, 3.14 mmol) was dissolved in 5 ml sulfuric acid and cooled at –5°C with salt–ice bath. A mixture of H<sub>2</sub>SO<sub>4</sub> (4 ml) and HNO<sub>3</sub> (4 ml) acid was prepared and the acid mixture was cooled at –5°C. The solution obtained was cooled at 0°C on a salt–ice bath for a few minutes. While the 8-methoxyquinoline (**16**) solution was stirred with a magnetic stirrer, the H<sub>2</sub>SO<sub>4</sub>/HNO<sub>3</sub> mixture was added dropwise with the aid of a Pasteur pipette within 1 hr so that the solution temperature does not exceed 0°C. After 2 hr, the reaction was finished, the reaction mixture was poured into crushed ice (30 g) in a beaker. After the ice melted, the mixture was extracted with CH<sub>2</sub>Cl<sub>2</sub> (5 × 20 ml). The organic phase was neutralized with aq NaHCO<sub>3</sub> (10%) solution and dried over Na<sub>2</sub>SO<sub>4</sub>. The solvent was removed in vacuo and filtrated over silica. Yellow-colored needle crystals were obtained as the sole product in a yield of 87% (0.25 g). Mp. 140–143°C. <sup>1</sup>H NMR (400 MHz, CDCl<sub>3</sub>, δ, ppm): δ<sub>H</sub> 9.22 (dd, *J*<sub>42</sub> = 1.6 Hz, *J*<sub>43</sub> = 8.8 Hz, 1H, H<sub>4</sub>), 9.17 (dd, *J*<sub>24</sub> = 1.6 Hz, *J*<sub>23</sub> = 4.0 Hz, 1H, H<sub>2</sub>), 8.89 (s, 1H, H<sub>6</sub>), 7.84 (dd, *J*<sub>32</sub> = 4.4 Hz, *J*<sub>34</sub> = 8.8 Hz, 1H, H<sub>3</sub>), and 4.58 (s, 3H, OMe). <sup>13</sup>C NMR (100 MHz, CDCl<sub>3</sub>, δ, ppm): δ<sub>C</sub> 155.8, 151.3, 142.9, 139.4, 139.1, 132.9, 126.0, 124.7, 121.1, and 65.3 (–OMe). IR (solid KBr, ν<sub>max</sub>, cm<sup>–1</sup>): 3,110, 3,085, 3,055, 2,960, 2,927, 1,607, 1,572, 1,518, 1,498, 1,467, 1,382, 1,318, 1,262, 1,239, 1,189, 1,160, 1,096, 987, 959, 909, 837, 798, 760, 716, 693, and 604. Anal. calcd. for C<sub>10</sub>H<sub>7</sub>N<sub>3</sub>O<sub>5</sub> (249.0386): C, 48.20%; H, 2.83%; N, 16.86%. Found: C, 48.27%; H, 2.79%; N, 16.80%.

#### 4.1.4 | Synthesis of 6,8-dimethoxy-1-nitroquinoline

6,8-Dimethoxyquinoline (**11**; 0.50 g, 2.64 mmol) was dissolved in 5 ml sulfuric acid and cooled at –5°C with salt–ice bath. A mixture of H<sub>2</sub>SO<sub>4</sub> (3 ml) and HNO<sub>3</sub> (3 ml) acid was prepared and the acid mixture was cooled at –5°C. The solution obtained was cooled at 0°C on a salt–ice bath for a few minutes. While the 6,8-dimethoxyquinoline (**11**) solution was stirred with a magnetic stirrer, the H<sub>2</sub>SO<sub>4</sub>/HNO<sub>3</sub> mixture was added dropwise with the aid of a Pasteur pipette within 1 hr so that the solution temperature does not exceed 0°C. After 1 hr, the reaction was finished, the reaction mixture was poured into crushed ice (30 g) in a beaker. After the ice melted, the mixture was extracted with CH<sub>2</sub>Cl<sub>2</sub> (5 × 20 ml). The organic phase was neutralized with aq NaHCO<sub>3</sub> (10%) solution and dried over Na<sub>2</sub>SO<sub>4</sub>. The solvent was removed in vacuo and filtrated over silica. Brown oil was obtained as the sole product in yield of 97% (0.30 g). <sup>1</sup>H NMR (400 MHz, dimethyl sulfoxide [DMSO]-*d*<sub>6</sub>, ppm): δ<sub>H</sub> 8.89 (d, *J*<sub>23</sub> = 4.4 Hz, 1, H<sub>2</sub>), 8.85 (d, *J*<sub>43</sub> = 8.8 Hz, 1H, H<sub>4</sub>), 7.94 (dd, *J*<sub>32</sub> = 5.2 Hz, *J*<sub>34</sub> = 8.4 Hz, 1H, H<sub>3</sub>), 7.27 (d, *J*<sub>57</sub> = 1.6 Hz, 1H, H<sub>5</sub>), 7.22 (d, *J*<sub>57</sub> = 2.0 Hz, 1H, H<sub>7</sub>), 4.10 (s, 3H, OMe), and 3.96 (s, 3H, OMe). <sup>13</sup>C NMR (100 MHz, DMSO-*d*<sub>6</sub>, ppm): δ<sub>C</sub> 160.2 (q), 152.4 (q), 143.2, 142.8, 134.5 (q), 131.1 (q), 123.5, 105.4, 98.6, 57.3 (OMe), and 56.6 (OMe). IR (solid KBr, ν<sub>max</sub>, cm<sup>–1</sup>): 3,005, 2,937, 2,838, 1,667, 1,613, 1,579, 1,501, 1,452, 1,382, 1,234, 1,212, 1,158, 1,135, 1,120, 1,049,

1,029, 998, 934, 868, 829, 784, 663, and 626. Anal. calcd. for  $C_{11}H_{11}N_2O_4$  (235.0713): C, 56.17%; H, 4.71%; N, 11.91%. Found: C, 56.23%; H, 4.79%; N, 11.86%.

#### 4.1.5 | Synthesis of 3,6,8-tribromo-5-nitroquinoline

A solution of 3,6,8-tribromoquinoline (**6**; 0.70 g, 1.913 mmol) in 5 ml of sulfuric acid was cooled at  $-5^{\circ}\text{C}$  in a salt-ice bath and treated cautiously with a solution of 50% nitric acid in 10 ml of sulfuric acid at  $-5^{\circ}\text{C}$  while the 3,6,8-tribromoquinoline (**6**) solution was stirred. After 1 hr in an ice bath, the red mixture was allowed to stand at room temperature. The red-colored solution was poured into crushed ice (30 g) in a beaker. After the ice melted, the mixture was extracted with  $\text{CH}_2\text{Cl}_2$  ( $5 \times 15$  ml). The organic phase was neutralized with aq  $\text{NaHCO}_3$  (10%) solution and dried over  $\text{Na}_2\text{SO}_4$ . The solvent was removed in vacuo. Yellow-colored needle crystals were obtained as the sole product in yield of 100% (0.78 g). M.p.  $215\text{--}216^{\circ}\text{C}$ .  $^1\text{H}$  NMR (400 MHz,  $\text{CDCl}_3$ ,  $\delta$ , ppm):  $\delta_{\text{H}}$  9.12 (d,  $^4J = 2.0$  Hz, 1 H, H-2), 8.33 (s, 1 H, H-7), and 8.24 (d,  $^4J = 2.0$  Hz, 1 H, H-4).  $^{13}\text{C}$  NMR (100 MHz,  $\text{CDCl}_3$ ,  $\delta$ , ppm):  $\delta_{\text{C}}$  153.9, 146.2, 142.1, 136.1, 131.8, 129.0, 122.5, 122.0, and 113.5. IR (solid KBr,  $\nu_{\text{max}}$ ,  $\text{cm}^{-1}$ ): 3,074, 2,956, 2,921, 1,663, 1,650, 1,550, 1,455, 1,349, 1,320, 1,080, 1,014, 934, 893, 871, 806, 783, 737, 675, and 617. Anal. calcd. for  $\text{C}_9\text{H}_3\text{Br}_3\text{N}_2\text{O}_2$  (407.7745): C, 26.31%; H, 0.74%; N, 6.82%. Found: C, 26.22%; H, 0.73%; N, 6.80%.

## 4.2 | Biological assays

### 4.2.1 | MTT cell proliferation assay

HT29 (human colorectal adenocarcinoma), HeLa (human cervix adenocarcinoma), MCF7 (human breast adenocarcinoma), A549 (human lung carcinoma), and Hep3B (human hepatocellular carcinoma) cancer cell lines, and FL (human amnion cells) normal cell line were maintained in a suitable medium containing fetal bovine serum and antibiotic solution. A cell suspension was adjusted at  $1 \times 10^6$  cells in 10 ml and 100  $\mu\text{l}$  was transferred into each well of culture plates. The compounds were dissolved in sterile DMSO at final concentrations of 10–200  $\mu\text{g}/\text{ml}$  and the cells were incubated at  $37^{\circ}\text{C}$  with 5%  $\text{CO}_2$  overnight. The antitumor activities of the compounds were determined using MTT cell proliferation assay. In MTT assay, the percent inhibitions of test and control molecules were determined. The percent inhibition was equal % inhibitions with the following formula:

$$\text{Inhibition}(\%) = (A_{\text{sample}} - A_{\text{control}}) / (A_{\text{control}}) \times 100,$$

where  $A_{\text{sample}}$  is the absorbance of treated cells and  $A_{\text{control}}$  is the absorbance of the untreated cells. The  $\text{IC}_{50}$  values of the compounds were obtained by using Excel software and noted in  $\mu\text{g}/\text{ml}$  at 95% confidence intervals. The dose-response parameters ( $\text{GI}_{50}$ , TGI, and

$\text{LC}_{50}$ ) were calculated according to the following formulas using Excel software. The growth inhibition of 50% ( $\text{GI}_{50}$ ) was calculated from the following equation:

$$[(\text{Ti} - \text{Tz}) / (\text{C} - \text{Tz})] \times 100 = 50.$$

This formula is the drug concentration resulting in a 50% reduction in the net growth increase in control cells during the drug incubation. The total growth inhibition (TGI) was calculated from  $\text{Ti} = \text{Tz}$ .  $\text{LC}_{50}$ , indicating a net loss of treated cells, was calculated from the following equation:

$$[(\text{Ti} - \text{Tz}) / \text{Tz}] \times 100 = -50.$$

### 4.2.2 | Cytotoxicity assay

The cytotoxic potentials of the compounds were determined by a cytosolic LDH measurement kit according to the manufacturer's procedures.<sup>[56]</sup> Briefly,  $5 \times 10^3$  cells were conveyed into each well as triplicates and exposed with  $\text{IC}_{50}$  concentrations of the compounds at  $37^{\circ}\text{C}$  with 5%  $\text{CO}_2$  overnight. The percentage of cytotoxicities was obtained by using the following equation:

$$[(\text{Experimental value} - \text{Low control}) / (\text{High control} - \text{Low control})] \times 100,$$

where the experimental value pertains to the cells treated with the test compound, the high control (maximum LDH release) means the 2% Triton X-100-treated cells, and the low control (spontaneous LDH release) are the untreated cells.

### 4.2.3 | DNA binding studies

The binding constants ( $K_b$ ) against calf thymus DNA and physiological interactions of disubstituted tacrine derivatives were examined by using UV-Vis spectroscopy technique. To prepare stock calf thymus DNA solution, 2.5 mg DNA was dissolved in 10.0 ml Tris-HCl buffer (20 mM Tris-HCl, 20 mM NaCl, pH 7.0) and stored at  $+4^{\circ}\text{C}$  for up to 7 days. The DNA concentration in solution was calculated by using  $\epsilon$  value ( $6,600 \text{ M}^{-1} \cdot \text{cm}^{-1}$  at 260 nm) that belongs to DNA. In addition, the purity of the calf thymus DNA solution was controlled with the help of a change of absorbance obtained from the ratio of  $A_{260}/A_{280}$ . As the value was equal to 1.87, the DNA was considered to be sufficiently pure. To obtain 25  $\mu\text{M}$  of a working solution, disubstituted tacrine derivatives were diluted with Tris-HCl buffer and then all of the compounds were incubated at  $24^{\circ}\text{C}$  for 30 min before the measurement. To ensure sufficient solubility in solution throughout measurement, a special solvent system (1:9 DMSO/Tris-HCl buffer) was prepared. Eight measurement points at room temperature for disubstituted tacrine derivatives were recorded by using 1-cm-path quartz cuvettes. The number of disubstituted tacrine derivatives was kept constant while increasing the CT-DNA concentrations (6.5–800  $\mu\text{M}$ ) in the UV absorption titrations.

#### 4.2.4 | Microdilution assay

The minimal inhibitory concentration (MIC) values of disubstituted tacrine derivatives toward some human bacterial strains, (Gram[+], *E. faecalis* ATCC 19433, *E. faecalis* ATCC 29212, *S. aureus* ATCC 25923, *S. aureus* ATCC 29213, and *S. aureus* ATCC 46300; Gram[-], *E. coli* ATCC 25922, *E. coli* ATCC 35213, and *P. eruginosa* ATCC 27853], were examined with the help of a microwell dilution method. According to this method, the inocula of bacteria were obtained using 12-hr LB broth cultures. The optical density at 600 nm (OD<sub>600</sub>) was adjusted to 0.08–0.1 and 0.5 McFarland bacterial suspensions were obtained. Each disubstituted tacrine derivative was dissolved in DMSO (20 mg/ml). A concentration gradient range of 7.81–1,000 µg/ml in uncovered microplate wells containing nutrient broth was made by using serial two-fold dilutions of these compounds. This plate was inoculated with bacteria and incubated at 35°C for 24 hr. At the end of this period, the growth of microorganisms was determined visually, and the point where no visible growth was accepted as the MIC.

#### 4.2.5 | Enzyme inhibition studies

Both hCA isoenzymes' inhibition effects of novel compounds were measured according to the method of Verpoorte et al.,<sup>[57]</sup> conforming to previous studies,<sup>[58,59]</sup> and recorded at 348 nm spectrophotometrically using *p*-nitrophenyl acetate substrate. On the contrary, the AChE inhibitory effect of novel compounds was determined according to the procedure of Ellman et al.,<sup>[60]</sup> conforming to previous studies,<sup>[61,62]</sup> and recorded at 412 nm spectrophotometrically using acetylthiocholine iodide as a substrate for the enzymatic reaction. The 5,5'-dithio-bis(2-nitrobenzoic) acid compound was used for the measurement of the AChE activity.

#### 4.2.6 | Statistical analysis

For the statistical analysis, SPSS (Statistical Package for Social Sciences) for Windows computer program was used and standard deviation, *p* value, using means, one-way analysis of variance were employed, followed by Tukey's test.

### 4.3 | Molecular docking studies

#### 4.3.1 | Molecular docking for enzyme inhibition

The quinoline derivatives substituted with a number of different functional groups were preoptimized with the GaussView 5.0.8 package program.<sup>[63]</sup> Molecular docking data were obtained using the DockingServer service of Virtua Pharmaceutical Research and Development Company.<sup>[64]</sup> Compounds 1–19 and target proteins selected from Protein Data Bank<sup>[65]</sup> were reoptimized in DockingServer and docked.

#### 4.3.2 | Dock computations for the anticancer effect of compound 10

X-ray structure coordinates for phospholipase C gamma 1 (PLCγ1) in complex with fibroblast growth factor receptor 2 (FGFR2) were obtained from Protein Data Bank (PDB ID: 5EG3).<sup>[53]</sup> Molecular docking studies were performed using AutoDock\_Vina v1.1.2.<sup>[66]</sup> Ligands and the receptor were prepared for docking by MGLTools v1.5.4, and the dock results were visualized by the same program.<sup>[67]</sup> Gasteiger partial atomic charges were assigned to the receptor as well as the ligand. Rotatable bonds in all ligands were kept flexible, whereas those of the receptor were kept rigid. Ligand and receptor coordinates prepared by MGLTools were saved in PDBQT form. A gridbox, with size 30 Å (X) × 25 Å (Y) × 28 Å (Z) and center coordinates 15.209 (X) × -24.299 (Y) × 8.2133 (Z), was used to implement dock computations. Parameters exhaustiveness = 8 and num\_modes = 10 were used for AutoDock Vina computations.

#### CONFLICT OF INTERESTS

The authors declare that there are no conflicts of interests.

#### ORCID

Salih Ökten  <http://orcid.org/0000-0001-9656-1803>

Ali Aydın  <http://orcid.org/0000-0002-9550-9111>

Ümit M. Koçyiğit  <http://orcid.org/0000-0001-8710-2912>

Osman Çakmak  <http://orcid.org/0000-0001-9293-5572>

Sultan Erkan  <http://orcid.org/0000-0001-6744-929X>

Çenk A. Andac  <http://orcid.org/0000-0002-4545-3500>

Parham Taslimi  <http://orcid.org/0000-0002-3171-0633>

İlhami Gülçin  <http://orcid.org/0000-0001-5993-1668>

#### REFERENCES

- [1] N. Kahrıman, V. Serdaroglu, K. Peker, A. Aydın, A. Usta, S. Fandaklı, N. Yaylı, *Bioorg. Chem.* **2019**, *83*, 580.
- [2] V. F. Roche *Foye's Principles of Medicinal Chemistry* (Eds: D. A. Williams, T. Lemke), Lippincott Williams & Wilkins, Baltimore, MD **2002**, p. 1199.
- [3] A. Aydın, N. Korkmaz, Ş. Tekin, A. Karadağ, *Turk. J. Biol.* **2014**, *38*, 948.
- [4] Y. Laras, V. Hugues, Y. Chandrasekaran, M. Blanchard-Desce, F. C. Acher, N. Pietrancosta, *J. Org. Chem.* **2012**, *77*, 8294.
- [5] M. F. El Shehry, M. M. Ghorab, S. Y. Abbas, E. A. Fayed, S. A. Shedid, Y. A. Ammar, *Eur. J. Med. Chem.* **2018**, *143*, 1463.
- [6] S. Ökten, O. Çakmak, R. Erenler, Ö. Yüce, Ş. Tekin, *Turk. J. Chem.* **2013**, *37*, 896.
- [7] S. Ökten, O. Çakmak, Ş. Tekin, *Turk. J. Clin. Lab.* **2017**, *8*, 152.
- [8] S. Ökten, O. Çakmak, Ş. Tekin, T. K. Köprülü, *Lett. Drug. Des. Discov.* **2017**, *14*, 1415.
- [9] I. Gonzalez-Sanchez, J. D. Solano, M. A. Loza-Mejia, S. Olvera-Vazquez, R. Rodriguez-Sotres, J. Moran, A. Lira-Rocha, M. A. Cerbon, *Eur. J. Med. Chem.* **2011**, *46*, 2102.
- [10] M. Mishra, V. Mishra, V. Kashaw, A. K. Iyer, S. K. Kashaw, *Eur. J. Med. Chem.* **2017**, *125*, 1300.
- [11] Y. Chai, M. L. Liu, K. Lv, L. S. Feng, S. J. Li, L. Y. Sun, S. Wang, H. Y. Guo, *Eur. J. Med. Chem.* **2011**, *46*, 4267.
- [12] O. Afzal, S. Kumar, M. R. Haider, M. R. Ali, R. Kumar, M. Jaggi, S. Bawa, *Eur. J. Med. Chem.* **2015**, *97*, 871.
- [13] H. Zhao, Y. Xing, P. Lu, Y. Wang, *Chem. Eur. J.* **2016**, *22*, 15144.

- [14] O. Çakmak, S. Ökten, *Tetrahedron* **2017**, *73*, 5389.
- [15] T. K. Köprülü, S. Ökten, Ş. Tekin, O. Çakmak, *J. Biochem. Mol. Toxicol.* **2019**, *33*, e22260.
- [16] S. Ökten, C. C. Ersanlı, O. Çakmak, *Cumhuriyet Sci. J.* **2018**, *39*, 940.
- [17] S. Ökten, *J. Chem. Res.* **2019**, *43*, 274.
- [18] L. Paloque, P. Verhaeghe, M. Casanova, C. Castera-Ducros, A. Dumètre, L. Mbatchesi, S. Hutter, M. Kraiem-Mrabet, M. Laget, V. Remusat, S. Rault, P. Rathelot, N. Azas, P. Vanelle, *Eur. J. Med. Chem.* **2012**, *54*, 75.
- [19] T. Nunoshiha, B. Demple, *Cancer Res.* **1993**, *53*, 3250.
- [20] O. Çakmak, S. Ökten, D. Alimli, A. Saddiqa, C. C. Ersanlı, *ARKIVOC* **2018**, *iii*, 362.
- [21] C. Q. Huang, K. Wilcoxon, J. R. McCarthy, M. Haddach, T. R. Webb, J. Gu, Y. F. Xie, D. E. Grigoriadis, C. Chen, *Bioorg. Med. Chem. Lett.* **2003**, *13*, 3375.
- [22] X. Wang, X. Xie, Y. Cai, X. Yang, J. Li, Y. Li, W. Chen, M. He, *Molecules* **2016**, *21*, 340.
- [23] A. Manikandan, S. Ravichandran, K. I. Sathiyarayanan, A. Sivakumar, *Inflammopharmacology* **2017**, *25*, 621.
- [24] A. T. Vu, S. T. Cohn, E. S. Manas, H. A. Harris, R. E. Mewshaw, *Bioorg. Med. Chem. Lett.* **2005**, *15*, 4520.
- [25] T. C. Ko, M. J. Hour, J. C. Lien, C. M. Teng, K. H. Lee, S. C. Kuo, L. J. Huang, *Bioorg. Med. Chem. Lett.* **2001**, *11*, 279.
- [26] K. Chen, S. C. Kuo, M. C. Hsieh, A. Mauger, C. M. Lin, E. Hamel, K. H. Lee, *J. Med. Chem.* **1997**, *40*, 3049.
- [27] Y. L. Chen, C. J. Huang, Z. Y. Huang, C. H. Tseng, F. S. Chang, S. H. Yang, S. R. Lin, C. C. Tzeng, *Bioorg. Med. Chem.* **2006**, *14*, 3098.
- [28] F. K. Abdel-Wadood, M. I. Abdel-Monem, A. M. Fahmy, A. A. Geies, *Arch. Pharm. Chem. Life Sci.* **2014**, *347*, 142.
- [29] A. Şahin, O. Çakmak, İ. Demirtaş, S. Ökten, A. Tutar, *Tetrahedron* **2008**, *64*, 10068.
- [30] S. Ökten, D. Eyigün, O. Çakmak, *Sigma J. Eng. Nat. Sci.* **2015**, *33*, 8.
- [31] P. Metrangolo, F. Meyer, T. Pilati, G. Resnati, G. Terraneo, *Angew. Chem. Int. Ed.* **2008**, *47*, 6114.
- [32] Z. Xu, Z. Yang, Y. Liu, Y. Lu, K. Chen, W. Zhu, *J. Chem. Inf. Model.* **2014**, *54*, 69.
- [33] D. M. Berger, M. Dutia, D. Powell, M. B. Floyd, N. Torres, R. Mallon, D. Wojciechowicz, S. Kim, L. Feldberg, K. Collins, I. Chaudhary, *Bioorg. Med. Chem.* **2008**, *16*, 9202.
- [34] F. F. Fleming, L. Yao, P. C. Ravikumar, L. Funk, B. C. Shook, *J. Med. Chem.* **2010**, *53*, 7902.
- [35] C. C. Cheng, S. J. Yan, *Org. React.* **1982**, *28*, 37.
- [36] M. Pauvert, S. C. Collet, A. M. J. Bertrand, A. Y. Guingant, M. Evain, *Tetrahedron Lett.* **2005**, *46*, 2983.
- [37] S. Martine, K. Evelyne, J.-P. Macher, B. Jean-Jacques, M. Abarghaz, P. Wagner, G. Ronsin, US Patent 183909, A1, 2006, Arlington, VA.
- [38] P. Charpentier, V. Lobregat, V. Levacher, G. Dupas, G. Queguiner, J. Bourguignon, *Tetrahedron Lett.* **1998**, *39*, 4013.
- [39] S. Ökten, O. Çakmak, *Tetrahedron Lett.* **2015**, *56*, 5337.
- [40] S. Ökten, O. Çakmak, A. Saddiqa, B. Keskin, S. Özdemir, M. Inal, *Org. Commun.* **2016**, *9*, 82.
- [41] S. Ökten, M. Ekiz, A. Tutar, Ü. M. Koçyiğit, B. Bütün, G. Topçu, İ. Gülçin, *Indian J. Pharm. Educ. Res.* **2019**, *53*, 268.
- [42] M. Ekiz, A. Tutar, S. Ökten, B. Bütün, Ü. M. Koçyiğit, P. Taslimi, G. Topçu, *Arch. Pharm. Chem. Life Sci.* **2018**, *351*, e1800167.
- [43] S. Ökten, M. Ekiz, Ü. M. Koçyiğit, A. Tutar, İ. Çelik, M. Akkurt, F. Gökalp, P. Taslimi, İ. Gülçin, *J. Mol. Struct.* **2019**, *1175*, 906.
- [44] M. J. Keiser, B. L. Roth, B. N. Armbruster, P. Ernsberger, J. J. Irwin, B. K. Shoichet, *Nat. Biotechnol.* **2007**, *25*, 197.
- [45] S. A. Eccles, *Curr. Opin. Genet. Dev.* **2005**, *15*, 77.
- [46] R. Lattanzio, M. Iezzi, G. Sala, N. Tinari, M. Falasca, S. Alberti, S. Buglioni, M. Mottolose, L. Perracchio, P. G. Natali, M. Piantelli, *BMC Cancer* **2019**, *19*, 747.
- [47] G. Sala, F. Dituri, C. Raimondi, S. Previdi, T. Maffucci, M. Mazzeletti, C. Rossi, M. Iezzi, R. Lattanzio, M. Piantelli, S. Iacobelli, M. Brogini, M. Falasca, *Cancer Res.* **2008**, *68*, 10187.
- [48] Y. R. Yang, J. H. Choi, J. S. Chang, H. M. Kwon, H. J. Jang, S. H. Ryu, P. G. Suh, *Adv. Biol. Regul.* **2012**, *52*, 138.
- [49] J. S. Lee, J. Kim, B. Y. Kim, H. S. Lee, J. S. Ahn, Y. S. Chang, *J. Nat. Prod.* **2000**, *63*, 753.
- [50] G. Trani, J. J. Barker, S. M. Bromidge, F. A. Brookfield, J. D. Burch, Y. Chen, C. Eigenbrot, A. Heifetz, M. H. A. Ismaili, A. Johnson, T. M. Krülle, C. H. MacKinnon, R. Maghames, P. A. McEwan, C. A. G. N. Montalbetti, D. F. Ortwine, Y. Pérez-Fuertes, D. G. Vaidya, X. Wang, A. A. Zarrin, Z. Pei, *Bioorg. Med. Chem. Lett.* **2014**, *24*, 5818.
- [51] L. Dai, X. Chen, X. Lu, F. Wang, Y. Zhan, G. Song, T. Hu, C. Xia, B. Zhang, *Sci. Rep.* **2017**, *7*, 13912.
- [52] T. D. Bunney, D. Esposito, C. Mas-Droux, E. Lamber, R. W. Baxendale, M. Martins, A. Cole, D. Svergun, P. C. Driscoll, M. Katan, *Structure* **2012**, *20*, 2062.
- [53] Z. Huang, W. M. Marsiglia, U. B. Roy, N. Rahimi, D. Ilghari, H. Wang, H. Chen, W. Gai, S. Blais, T. A. Neubert, A. Mansukhani, N. J. Traaseth, X. Li, M. Mohammadi, *Mol. Cell* **2016**, *61*, 98.
- [54] İ. Çelik, M. Akkurt, S. Ökten, O. Çakmak, S. Garcia-Granda, *Acta Crystallogr. Sect. E* **2010**, *E66*, o3133.
- [55] İ. Çelik, S. Ökten, C. C. Ersanlı, M. Akkurt, O. Çakmak, R. Özbakır, *IUCrData* **2017**, *2*, 170643.
- [56] S. Ökten, R. Erenler, T. K. Köprülü, Ş. Tekin, *Turk. J. Biol.* **2015**, *39*, 15.
- [57] J. A. Verpoorte, S. Mehta, J. T. Edsall, *J. Biol. Chem.* **1967**, *242*, 4221.
- [58] M. Huseynova, P. Taslimi, A. Medjidov, V. Farzaliyev, M. Aliyeva, G. Gondolova, O. Şahin, B. Yalçın, A. Sujayev, E. B. Orman, A. R. Özkaya, İ. Gülçin, *Polyhedron* **2018**, *155*, 25.
- [59] A. Biçer, P. Taslimi, G. Yakalı, İ. Gülçin, M. S. Gültekin, G. T. Cin, *Bioorg. Chem.* **2019**, *82*, 393.
- [60] G. L. Ellman, K. D. Courtney, V. Andres, R. M. Featherston, *Biochem. Pharmacol.* **1961**, *7*, 88.
- [61] B. Yiğit, R. Kaya, P. Taslimi, Y. Işık, M. Karaman, M. Yiğit, İ. Özdemir, İ. Gülçin, *J. Mol. Struct.* **2019**, *1179*, 709.
- [62] Ç. Bayrak, P. Taslimi, H. S. Kahraman, İ. Gülçin, A. Menzek, *Bioorg. Chem.* **2019**, *85*, 128.
- [63] R. D. Dennigton II, T. A. Keith, J. M. Millam, *GaussView 5.0*, Gaussian, Inc., Wallingford, CT **2009**.
- [64] K. Sayin, D. Karakaş, S. E. Kariper, T. A. Sayin, *J. Mol. Struct.* **2018**, *1156*, 172.
- [65] PDB (Protein Data Bank); <http://www.rcsb.org/pdb/>; last accessed: 01 March 2020.
- [66] O. Trott, A. J. Olson, *J. Comput. Chem.* **2010**, *31*, 455.
- [67] G. M. Morris, R. Huey, W. Lindstrom, M. F. Sanner, R. K. Belew, D. S. Goodsell, A. J. Olson, *J. Comput. Chem.* **2009**, *16*, 2785.

## SUPPORTING INFORMATION

Additional supporting information may be found online in the Supporting Information section.

**How to cite this article:** Ökten S, Aydın A, Koçyiğit ÜM, et al. Quinoline-based promising anticancer and antibacterial agents, and some metabolic enzyme inhibitors. *Arch Pharm.* 2020;e2000086. <https://doi.org/10.1002/ardp.202000086>